Toxic Oligomeric Variants of TDP-43 May Contribute to Cognitive Deficits Secondary to Diffuse Experimental TBI

by

Umar Syed Aftab

A Thesis Presented in Partial Fulfillment
of the Requirements for the Degree
Master of Science

Approved July 2021 by the
Graduate Supervisory Committee:

Michael Sierks, Co-Chair
Rachel K. Rowe, Co-Chair
Jason M. Newbern

ARIZONA STATE UNIVERSITY

August 2021

ABSTRACT

Traumatic Brain Injury (TBI) affects approximately two million people on an annual basis and increases the frequency and onset of Alzheimer's disease (AD) and other related dementias (ADRDs). Mechanical damage and shearing of neuronal axons are thought to be responsible for producing toxic variants of proteins that contribute to disease pathology. Specifically, the tau, beta amyloid, alpha-synuclein, and TAR-binding DNA Protein-43 (TDP-43) variants contribute to the heterogenous pathology mechanisms of neurodegenerative diseases. The Sierks lab at Arizona State University has aimed to study how these protein variants collectively interact to contribute to pathologies characteristic of AD/ADRDs. This study focuses on the accumulation of toxic oligomeric variants of TDP-43 secondary to TBI. The first aim of this study was to identify the protein variant fingerprint as a function time following experimental diffuse TBI. The second aim was to investigate if toxic variants of TDP-43 were associated with cognitive and motor functional deficits. C57BL/6 mice were subjected to a single or repetitive diffuse TBI via midline fluid percussion injury or a control surgery (sham). Post-injury, mice were evaluated for cognitive performance, sensorimotor function, and depressive-like behavior at 7-, 14-, and 28-days post-injury. Tissue was collected for immunohistochemistry and stained for ADTDP-3, a single chain antibody variable fragment (ScFv) which binds to toxic variants of TDP-43 in amyotrophic lateral sclerosis (ALS) and AD tissue. A one-way analysis of variance (ANOVA) was performed to compare staining intensity across various brain regions. Subsequently, a Pearson correlation was performed to compare behavioral task performance to staining intensity by brain region for each injury group. There were

significantly elevated levels of ADTDP3 binding in all regions except for the hippocampus, and there was a significant correlation between the cortex staining intensity vs the cognitive behavior test at 7 days post-injury. There was also a significant correlation between the thalamus staining intensity and sensorimotor test at 7 days post-injury. These findings support the hypothesis that the accumulation of toxic variants of TDP-43 can contribute to neurodegenerative pathology and loss of function. These variants also may contribute to behavioral deficits secondary to diffuse TBI.

ACKNOWLEDGMENTS

I am indebted to my defense committee for their feedback and challenges to my thinking. I am grateful to both of my co-chairs, Dr. Michael Sierks and Dr. Rachel Rowe, for allowing me to work on this collaborative project for my Master's thesis. I'm grateful to the Rowe lab and to the rest of the Translational Neurotrauma Research Program at the University of Arizona College of Medicine-Phoenix for the integral role they have played in my development as a scientific researcher and a student of biology. Dr. Rachel Rowe, Dr. J. Bryce Ortiz, Dr. Jonathan Lifshitz, Tabitha Green, Katie Giordano, and Yerina Hur were especially crucial to my intellectual growth. I'm grateful to the Sierks lab at Arizona State University for facilitating my project over this last year despite the difficulties and challenges posed by the COVID-19 pandemic. I'm especially thankful to Dr. Michael Sierks, Phil Schulz, Nick Panayi, and Ping for all their contributions and help. Despite all the unique challenges this pandemic-ridden year offered, I could not be more content with my experiences in the Sierks lab. I am grateful to my third defense committee member, Dr. Jason Newbern, for all his rigorous feedback and questioning throughout this process.

TABLE OF CONTENTS

CHAPTER Page

CHAPTER 1

INTRODUCTION

Traumatic Brain Injury

Traumatic brain injury (TBI) results from a sudden impact or acceleration trauma to the head that causes neuropathologic damage or dysfunction—and is a major cause of death and disability on an annual basis worldwide (McKee, 2015). More specifically, TBI is defined as a nondegenerative, non-congenital injury to the brain occurring *via* an extraneous physical strength that may result in impaired or changed level of consciousness, leading to permanent or temporary disabilities of cognitive or physical functioning (Pavlova et al., 2018). According to the Center for Disease Control and Prevention (CDC), approximately 2.87 million cases of TBI occur in the U.S. annually, with an estimated 837,000 of these being children (Agarwal et al.). Of these cases, it is estimated that around 50,000 die from TBI each year, and around 80,000-90,000 individuals experience the onset of long-term or lifelong disabilities each year (Agarwal et al.). The most common mechanisms for disease include falls, motor vehicle crashes, assault, domestic violence, and suicide (Agarwal et al.). War and civil unrest are also a significant contributor to TBI cases on a global scale (Champion et al., 2009). TBI has been named the "signature wound" of current conflicts in Iraq and Afghanistan by the U.S. Department of Veteran Affairs War Related Illness and Injury Study Center (Champion et al., 2009). Efforts to quantify the magnitude of TBI both nationally and globally are severely hampered—which suggests that these values could be greatly underestimated. Mild TBI is difficult to capture, and subsequent medical treatment for mild TBIs are often not sought after. Another reason for the probable underreporting of TBI is due to its silent nature and the absence of injury

surveillance or reporting systems throughout the world. These high incidence rates coupled with probable underreporting creates a pressing public health and medical issue globally (Hyder et al., 2007).

As medical research in the TBI field has progressed, the scientific community's understanding of TBI as a disease has gradually evolved. Once understood as a "single injury event", TBIs are now viewed as dynamic events with complex and heterogenous mechanisms. The generally accepted consensus understanding of TBI today is one of a *progressive* disease which can be stimulated or induced by numerous events or occurrences over time (Blennow et al., 2016). The modern prevailing view of TBI is that TBI is a dynamic condition that continue to change after years of onset, where many individuals who endure such injuries experience cognitive decline over time due to progressive, neurodegenerative processes, comorbid conditions, behavioral choices, and/or psychosocial factors (Blennow et al., 2016). TBI's unique heterogeneity is further complicated by the possibility of repetitive TBI (rTBI). In a literature review, Fehily and Fitzgerald showed that rTBI can exacerbate metabolic dysregulation and oxidative stress compared to single TBI groups (Fehily and Fitzgerald, 2017). Furthermore, Fehily and Fitzgerald showed that astroglia and microglia proliferate at a greater rate and are sustained longer in rTBIs—which can significantly alter both short-term and long-term pathology (Fehily and Fitzgerald, 2017). This further emphasizes a critical need to understand TBI on a comprehensive level, where morbidity analysis synthesizes molecular, structural, functional, and behavioral elements to develop targeted treatments accordingly.

There are varying types of TBI that must be taken into consideration. Generally, the three classifications for TBI include focal injury, diffuse injury, and blast injury (Hamdeh et al., 2018). Focal brain damage is produced by collision forces acting on the skull, resulting in compression of the tissue underneath the cranium at the site of impact (coup) or of tissue oppositely to the impact (contre-coup). This contrecoup-coup phenomenon is hypothesized to induce brain damage because the *in vivo* brain is less dense than the cerebrospinal fluid (CSF), and the denser CSF moves towards the site of skull impact—displacing the brain in the opposite direction such that the initial impact of the brain parenchyma is at the contrecoup location (Drew, 2004). The differential biomechanics of a focal injury cause vastly different phenotypes when compared with its diffuse and blast injury counterparts. Focal injuries constitute subdural and epidural hematomas, intraparenchymal hematomas and (hemorrhagic) contusions (Andriessen et al., 2010). On the other hand, diffuse TBI phenotypes include widely distributed damage to axons, diffuse vascular injury, hypoxic-ischemic injury, and brain swelling (edema). The main injury mechanism responsible for diffuse injury is rapid acceleration–deceleration of the head, as seen, for example in high-speed motor-vehicle accident (Andriessen et al., 2010). Diffuse Axonal Injury (DAI) is the predominant mechanism of injury for diffuse TBI. The principal anatomic sites for DAI are most often the parasagittal white matter of the cerebral cortex, corpus callosum, and the pontine-mesencephalic junction adjacent to the superior cerebellar peduncles. The molecular features of DAI correspond to Wallerian-type axonal degeneration, and it is theorized that direct intracellular injury occurs from mechanical displacement of the cytoskeleton and cytoplasm (Meythaler et al., 2001). This

can be further exacerbated by the cascade of biochemical events that follow in the immunological response to DAI (Meythaler et al., 2001). Diffuse TBIs constitute the vast majority of TBI cases, and DAI is one of the most common TBI phenotypes (Povlishock and Katz, 2005). Blast injuries—the "signature wound" of the Afghanistan and Iraq wars—are traumatic neurological injuries due to blast exposure and are largely attributed to explosive devices in terrorist and insurgent activities (Bryden et al., 2019). Mechanistically, the explosion energy outside the body is transformed into biokinetic energy that causes damage to the brain and structures of the cranium from the overpressure. The resulting damage that this mechanical energy causes is similar to blunt causes of TBI. Severe cases of blunt TBI are heterogenous in their nature, and the nature of blast injury adds an additional layer of complexity (Bryden et al., 2019).

Pathophysiology of TBI

When constructing the framework to analyze TBI from a temporal view, it is important to separate the order of injury into two phases—the primary phase and the secondary phase. Briefly, the distinction between primary and secondary injury is that primary injury (focal, diffuse, or blast) results in mechanical injury or trauma, while the secondary injury is caused by the body's physiological response to the primary injury (Pearn et al., 2017). This distinction was well illustrated in the previously mentioned example of DAI, and how the mechanical stress induced by the injury (primary phase) is often further exacerbated by the following cascade of biochemical events (secondary phase) (Pearn et al., 2017). To elaborate on this further, there are distinct categorical effects caused by each of these responses. Primary phase is generally characterized by the

mechanical shearing of axons and blood vessels. This often results in conspicuous phenotypes, including nonspecific neuronal cell damage and death (caused by the shearing of tissues via the kinetic energy deposited on impact), diffuse axonal injury, and synaptic disruption (Aniessen et al., 2010). Secondary injury is classified as microvascular and neuronal injury due to a cascade of pathophysiological events that further exacerbate the primary injury. On a molecular and cellular level, the secondary phase is characterized by the formation of free radicals (which can cause oxidative damage and create toxic protein variants), metabolic dysregulation, and glial cell activation (a customary part of the neuroimmunological response to injury but can also cause injury such scarring) (Pearn et al., 2017). The interrelationship between these phenotypes must also be illustrated to demonstrate the unique heterogeneity of TBI as a disease. For example, metabolic dysregulation is directly linked to activation/repression of hypoxia inducible factor (HIF)—which can increase reactive oxygen species formation via NADPH oxidase (Chen et al., 2018). The formation of free radicals subsequent to primary injury is of particular concern, as this has frequently been the hypothesized mechanism for toxic variant proteins that present in neurodegenerative disorders like Alzheimer's Disease (Iguchi et al., 2012). There is extensive evidence in the literature to show that oxidative stress stemming from metabolic dysfunction—such as glutathione depletion—can produce pathological modifications to TDP-43: a major component of ubiquitin-positive inclusion of TDP-43 proteinopathies including amyotrophic lateral sclerosis and frontotemporal lobar degeneration with ubiquitinated inclusions (Iguchi et al., 2012).

To explore the pathophysiology of TBI on a molecular and cellular level, it is helpful to illustrate a temporal landscape of events. The immediate effect subsequent to the primary phase is the induced porosity of the blood-brain barrier (BBB)—a critical element of the neuroinflammation that stems from primary injury (Needham et al., 2019). The induced porosity of the BBB allows for pro-inflammatory cytokines such as interferon γ (IFNγ), interleukin-2 (IL-2), and others necessary to facilitate the immune response to enter the CNS and various regions of damage (Petty, 2002). The aforementioned nonspecific neuronal death from the primary phase results in the accumulation of cellular debris that needs to be cleared. The presence of cellular debris activates the neuroimmunological response. Specifically, the mechanical damage induced to neuronal cells causes release of cellular debris—or DAMPs (damage-associated-molecular-patterns)—which systemically induce an immune response through microglial activation and subsequent astrogliosis (Needham et al., 2019). These immunological responses may exist to restore homeostasis for the damaged tissue, but they are also inadvertently responsible for the injuries of the secondary phase (Needham et al., 2019).

Another repercussion of this temporary porosity of the BBB is that it allows for infiltration of blood-borne factors and proteins that otherwise would be unable to access the central nervous system. For example, Blixt and colleagues were able to show a 20% elevation in levels of IgG permeability in accordance with a BBB breakdown, congruent with a decrease of a tight junction protein called Zona Occuldens-1 (Blixt et al, 2015). Notably, the development of this secondary brain injury presents a window where pharmaceutical compounds and neuro-rehabilitative properties can be administered

without inhibition from the blood brain barrier, so this properly can be utilized for engineering therapeutic advantages as well.

It is also worth evaluating the timeline of BBB breakdown chronologically. As mentioned previously, this period of BBB porosity represents a critical period where drugs can be administered to enter the brain without BBB inhibition. The vast amount of literature on this topic indicates this period of BBB fluidity and permeability only lasts for the first several days immediately subsequent to the injury. For example, Bao and colleagues (2012) found cerebral water content (CWC) was at its highest 24-48 hours post-TBI, up to 72 hours post-TBI before returning normal levels (Bao et al, 2012).

Illustrating the timeline of TBI pathophysiology on a molecular scale helps underscore how complex and heterogenous of a disease it is. The primary phase is the mechanical shearing of axons and blood vessels, and the body's immunological response mechanisms are capable of altering and exacerbating the injuries in a variety of ways. The creation of toxic protein variants from metabolic dysregulation, excitotoxicity from cell membrane damage, general inflammation, and cellular infiltrate from a leaky BBB are collectively capable of creating unique TBIs on an individual basis. This unique heterogeneity has made pharmaceutical development and therapeutic treatment difficult in the past, which only emphasizes the need to study it further.

Alzheimer's Disease and Related Diseases

According to the Joint Program of Neurodegeneration (JPND) research, "Neurodegenerative disease" is an umbrella term to describe a range of conditions which are primarily characterized by neuronal death or dysfunction later in life (Mayeux, 2003).

These diseases tend to be incurable and debilitating conditions that result in progressive degeneration of neurons, with the most common behavioral deficits being ataxia (movement dysfunction) and dementia (mental dysfunctions). Some of the most common neurodegenerative diseases include Parkinson's Disease (PD), Alzheimer's Disease (AD), Frontotemporal Dementia (FD), and Huntington's Disease (HD) (Mayeux, 2003). Despite differences in their defining clinical manifestations, the neurological diseases share several features: onset during middle age or in the later years of life, occurrence as either an inherited or sporadic disorder, and the intra- or extracellular aggregation and deposition of altered proteins (Mayeux, 2003).

A major public health concern is the anticipated increase of neurodegenerative diseases such as AD and ADRDs in the coming decades, as the number of older adults will continue to rise in the ensuing decades. For example, an estimated 6.2 million Americans of ages 65 and older are living with AD today, but the projected number of AD cases for Americans over the age of 65 by 2050 is a staggering 12.7 million (Alzheimer's Association, 2021). The social costs of this aging population are clear and will further exacerbate the strain already placed on healthcare systems, caregivers, and society at large. Age is the most significant risk factor for AD, with a vast majority of people who develop AD being aged 65 or older. While only 3% of the AD popular falls within the 65-74 age range, 17% falls within the 75-84 age range and 32% of people aged 85 and older have AD. It is important to make the distinction that diseases like AD are not a "natural" part of aging, as older age alone is not thought to be a sufficient cause of dementia (Gaugler et al., 2018).

The diagnostic guidelines for AD have also evolved as the science on the topic has progressed. In 1984, only individuals with measurable symptoms of learning, thinking, or memory disabilities could satisfy the criteria for AD. However, 2011 guidelines allow for diagnosis of AD if there are brain changes identified prior to the onset of symptoms. The 2011 guidelines build upon research that suggests that AD encompasses a continuum that begins with the initial brain changes of AD that start years before symptoms appear, continuing with years of symptoms that affect cognitive and physical function, and ending with severe AD, when brain changes are so extensive that individuals can no longer walk and struggle to communicate (Braak et al., 1997). This result has shifted the clinical criteria of the phenotype formerly called "Alzheimer's Disease in 1984 to "Alzheimer's Dementia" today (Braak et al., 1997).

Pathophysiology of Alzheimer's Disease

TAR-DNA Binding Protein 43

Transactive response (TAR) DNA Binding Protein 43 (TDP-43) is a protein coded by the *TARDBP* gene and is a member of the heterogenous ribonucleoprotein family (hnRNP) (Buratti E, Baralle FE., 2010). HnRNPs are involved in most gene expression pathways, from DNA replication to mRNA translation (Buratti E, Baralle FE., 2010). TDP-43 is normally expressed in the nucleus of neurons, where its primary function is to regulate RNA processing by binding to UG-rich introns in a customary RNA splicing mechanism (Tollervey et al., 2011). TDP-43 has also been shown to play a positive role in exon inclusion during the splicing of certain genes. Less studied but identified mechanisms of

TDP-43 include neurofilament stability, stress granule formation, mRNA translation, and potentially snoRNA metabolism (Buratti E, Baralle FE., 2010).

The perceived involvement of TDP-43 in neurodegeneration has been studied extensively throughout the past few decades, and there is now an emerging consensus that TDP-43 protein is mechanistically linked to neurodegeneration (Lee, Lee, & Trojanowksi, 2012). TDP-43 has been identified as a major constituent of the proteinaceous inclusions which are characteristic of most forms of amyotrophic lateral sclerosis (ALS) and frontotemporal degeneration (FTD). Despite distinct clinical differences, ALS and FTD have been thought of as related disorders. There is strong molecular biology-driven evidence to support this relationship, as TDP-43 has been shown to be the main protein constituent of ubiquitin-positive inclusions observed in the majority of ALS and FTD patients (Vanden Broeck L, Callaerts P, Dermaut B, 2013). Although TDP-43 is generally understood to be a nuclear protein, aggregates of TDP-43 have been shown to relocate to the cytoplasm in histological stains of FTD, ALS, and AD brain tissue (Vanden Broeck L, Callaerts P, Dermaut B, 2013). The functions of these TDP-43 aggregates in contributing to these pathologies are still unknown, but there are a few hypotheses that aim to explain how cytoplasmic TDP-43 aggregation can contribute to disease. Vanden Broek and colleagues acknowledge both gain-of-function and loss-of-function possibilities (Vanden Broeck L, Callaerts P, Dermaut B, 2013). TDP-43 is an evolutionary conserved protein, so a variety of animal models have been produced to test these hypotheses. Some of these models have overexpressed the *TARDBP* gene and consistently found ALS-FTD disease phenotypes (Vanden Broeck L, Callaerts P, Dermaut B, 2013). However, these models

have not shown cytoplasmic accumulation or nuclear depletion of TDP-43 (Rohn et al., 2009). On the contrary, there is substantially more evidence for loss-of-function hypothesis. For example, a study in Drosophila knocking out dTDP-43—Drosophila's ortholog to human TDP-43—led to decreased synaptic transmission which progressed to neurodegeneration (Vanden Broeck L, Callaerts P, Dermaut B, 2013).

Other Notable Biomarkers

Tau proteins—which are microtubule binding proteins that facilitate axonal stability and are found ubiquitously throughout the central nervous system—are evidenced to be at the center of several pathologies involving microtubule and axonal dysfunction. There are six highly soluble isoforms of the tau protein—all products of the MAPT gene (Paglini et al., 2000). Tau is the major protein constituent to the formation of a distinctive neurodegenerative phenotype called "neurofibrillary tangles"—one of two major pathological hallmarks of AD (Paglini et al., 2000). Subsequent studies have found that tau aggregates are the primary pathological feature of clinically heterogeneous neurodegenerative disorders that are now collectively termed "tauopathies" (Paglini et al., 2000). These disorders include AD, progressive supranuclear palsy, corticobasal syndrome, some frontotemporal dementias, and chronic traumatic encephalopathy (CTE) (Orr, Miranda E. et al., 2017). All these progressive neurodegenerative disorders are pathologically defined by tau-positive deposits in the brain (Orr, Miranda E. et al., 2017). These tauopathies appear as insoluble twisted fibers consisting mostly of misfolded or hyperphosphorylated tau aggregates. However, there are notable subtle differences in the histology of neurofibrillary tangles depending on the neurodegenerative disease. To

explore the molecular underpinnings of these neurofibrillary tangles, Liu and colleagues demonstrated that human brain tau is modified by O-glycosylation, where the monosaccharide B-N-acetylglucosamine (GlcNac) attaches to serine/threonine residues via an O-linked glycosidic bond (Liu et al., 2004). Specifically, they showed that O-glycosylation regulates phosphorylation of tau in a site-specific manner both *in vitro* and *in vivo* (Liu et al., 2004). Most of these sites showed negative regulation, and the O-GlcNAcylation level in AD brains was significantly decreased when compared to wild type counterparts (Liu et al., 2004). These findings are significant because they illustrate a potential molecular mechanism for this hyperphosphorylated tau-aggregate phenotype that produces these neurofibrillary tangles. Additionally, the correlation of reduced O-GlcNAcylation with hyperphosphorylated tau provides an area for further investigation (Liu et al., 2004).

Microtubule function is mechanistically complex and has a variety of contributing factors. These loosely assorted groups of variables, called microtubule associated proteins (MAPs), all need to be considered. Although tau is thought to be the MAP most contributory to this neurofibrillary tangle pathology. For example, the phosphorylation of tau reduces its affinity for microtubules and its ability to promote microtubule polymerization—leading to overall microtubule instability (Ramkumar, Jong, McKenney, 2018). Phosphorylation at specific sites like Y18 regulates the dynamicity of tau on the microtubule and can affect the mobility of motor proteins like kinesin—showing that tau dysfunction can have complex downstream effects related to molecular motors (Ramkumar, Jong, McKenney, 2018).

Preliminary Studies

The Sierks lab at Arizona State University has focused on the generation of single-chain variable fragments (scFvs) that selectively recognize different toxic oligomeric variants of proteins that have been shown to be at the center of neurodegenerative pathologies like ALS, AD, FTD, and other ADRDs (Williams et al., 2017). These scFvs have been designed to readily distinguish between human AD and control brain tissue, cerebrospinal fluid (CSF), and sera samples. These scFvs were prepared using a biopanning protocol aimed to isolate morphology-specific reagents against TDP-43 variants in ALS by using a two-phase AFM-based radio-panning technology (Williams et al., 2017).

This was accomplished by subjecting a diverse phage library to multiple rounds of negative panning against off-target antigens using immune-tubes. Negative panning was performed sequentially against bovine serum albumin (BSA) aggregated TDP-43 and healthy human brain tissue. The following step was to perform AFM verification after each set of negative panning to ensure that all unwanted phages are removed. AFM is a scanning probe microscopy that allows for topographic imaging at a scale of nanometers. The extreme precision of this tool makes it an effective candidate for recognizing all unwanted phages. Additionally, AFM can provide insight into specific molecular features and interactions between biochemical residues of interest. This allows it to be used to monitor the progress of biopanning to confirm the specificity of these clones. After immunoprecipitating TDP-43 proteins from the homogenized motor cortex of ALS/FTD tissue and control cases using a commercially available polyclonal anti-TDP-43 antibody, it was found that 23 different complete scFv sequences preferentially bind ALS tissue over both FTD and healthy samples using phage ELISAs (Williams et al., 2017).

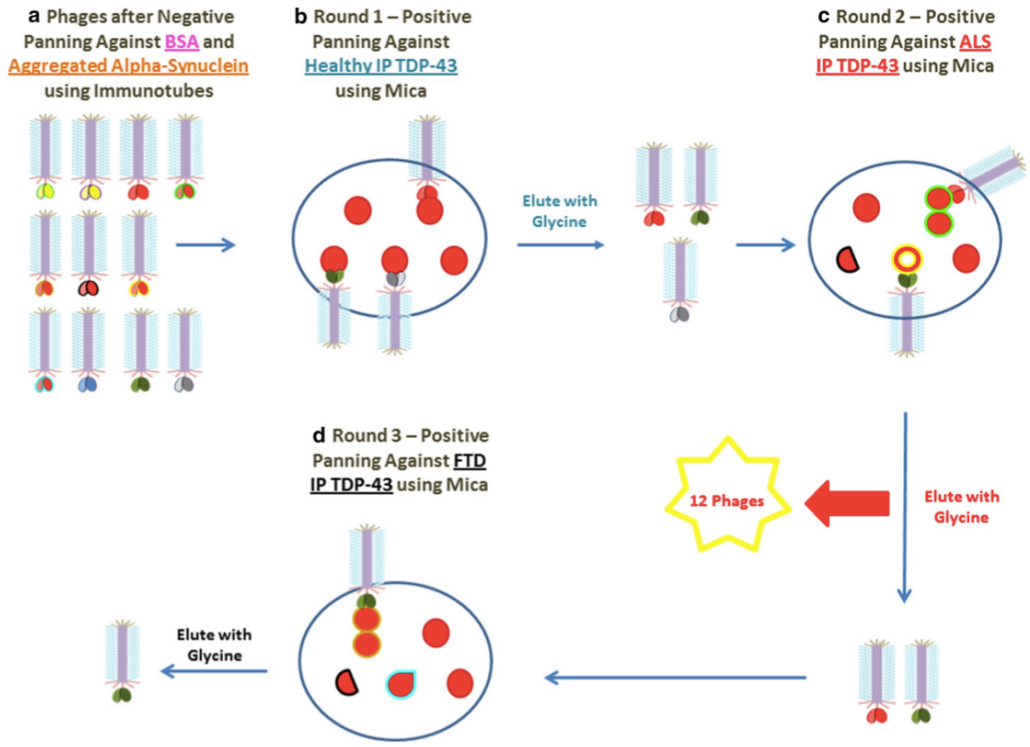

Figure 1: Schematic illustrating biopanning protocol to generate TDP-43 detection phages. A) All phage particles that bind to non-desired targets including BSA and aggregated alpha-synuclein are isolated and eliminated via immunotubes. **B)** Remaining phage particles from library are added to a mica surface containing TDP-43, which was immunoprecipitated from the motor cortex of healthy brain tissue. Glycine elution was used to elute bound phages so they could be added to **C)** a mica surface with TDP-43 immunoprecipitated from ALS brain tissue. (Williams et al., 2017) **D)** Final round of positive panning against FTD TDP-43 using mica. Not shown—fourth round of positive panning against AD brain tissue (occurred after publication of Williams et al., 2017).

Utilizing this biopanning protocol, numerous scFvs against toxic oligomeric variants found in neurodegenerative tissue have been developed. ScFvs that bind with specificity to toxic variants of TDP-43 in AD tissue include: ADTDP1, ADTDP2, and ADTDP3. Of these, ADTDP3 preferentially binds earlier-stage samples, while the other two preferentially bind late-stage samples.

TBI is known to increase neuronal stress through the various aforementioned methods, and environmental stress is known to be a significant factor in driving the

molecular pathologies of these neurodegenerative diseases. The Sierks lab has previously demonstrated that variants of these four proteins can be detected in veterans who have incurred TBI, but not in age matched veterans without TBI. These findings have led to the hypothesis that TBI results in the accumulation of toxic variants of TDP-43 that actively contribute to pathology and loss of function which can increase the risk of AD and ADRD. This hypothesis will be tested with the following Specific Aims:

Specific Aims

Specific Aim 1: To identify the AD/ADRD-related protein variant fingerprint as a function of sex and time following experimental diffuse traumatic brain injury.

Specific Aim 2: To investigate if toxic variants of TDP-43 accumulate in brain tissue and correlate with cognitive and motor function deficits.

CHAPTER 2

METHODS

Animals

C57BL/6 mice (two to four months of age) were used in this study (n=53). Mice were housed in 14hr light: 10hr dark cycle at constant temperatures (23 ± 2ºC) with food and water available *ad libitum*, according to the Association for Assessment and Accreditation of Laboratory Animal Care International. Mice were acclimated to their environment for one week before any experiments took place. Blocked randomization was used to assign mice to their respective treatment groups prior to the study. Specifically, they were assigned to the following groups: Sham, one hit, two hits three hours apart, and two hits nine hours apart. For histological analysis on a temporal landscape, a subset of animals from each group were euthanized at 7-, 14-, and 28-days post-injury (n=39 total). All procedures and animal care were conducted in compliance with Institutional Animal Care and Use Committee (IACUC) protocol 13-460 at the University of Arizona College of Medicine-Phoenix.

Midline Fluid Percussion Injury Model (mFPI)

Mice were subjected to moderate midline fluid percussion injury (mFPI) or a control sham surgery (where the craniectomy surgery was performed but no fluid percussion injury was induced) based on previously published methods (Rowe et al, 2018). To begin the procedure, mice were anesthetized using 5% isoflurane in 100% oxygen for five-minutes, mice were weighted, and placed into a stereotaxic frame (Kopf Instruments, Tujunga, CA) with continuously delivered isoflurane at 2.5 %. Throughout this procedure,

body temperature was monitored and maintained using an isothermal heating pad. Next, a midline scalp incision was performed followed by clamping to retract the skin and expose the surgical site. A 3.0 mm circular craniectomy was centered on the sagittal suture between bregma and lambda carefully ensuring that the underlying dura and superior sagittal sinus remained intact. An injury hub made from the female portion of a 20-gauge Luer-Loc needle was cut and beveled and fixed over the craniectomy using cyanoacrylate gel and methyl-methacrylate. The incision was sutured at the anterior and posterior edges, and the mice were returned to a heated recovery cage until ambulatory.

Approximately 24 hours following surgery, mice were re-anesthetized using 5% isoflurane in 100% oxygen for 3 minutes. The craniectomy was inspected and the status of the dura was noted to ensure no hemorrhaging had occurred. After the return of the pedal withdrawal response, a moderate injury was administered by attaching the male end of the hub to the fluid percussion device using extension tubing (#2c5643; Baxter, Deerfield , IL) and releasing the pendulum onto the fluid-filled cylinder. Shams were attached to the injury device, but the pendulum was not released. The injury hub was then removed, and the craniectomy was again inspected for herniation or hemorrhaging of the dura and the incision was sutured. Mice were monitored for the fencing response upon impact, changes in respiration rates, and the return of the righting reflex (Rowe et al., 2018).

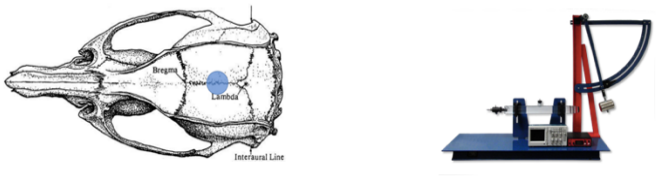

Figure 2: Midline Fluid Percussion Injury. **A)** Anatomical depiction of midline brain injury. Blue dot indicates where hub is placed during craniectomy surgery. **B)** Fluid percussion injury device. Pendulum is pulled back and released on the fluid-filled cylinder. Upon release, fluid pulse is sent through tub into intracranial hub to induce diffuse injury (Rowe et al., 2018)

A consideration to ensure that a diffuse injury was induced was to monitor for the fencing response—where the forearms are held flexed in the air and extended for several seconds immediately following a TBI—along with apnea. The fencing response is indicative of a diffuse injury since it provides qualitative evidence that the midline induced injury replicated a phenotype indicative of moderate force applied to the midbrain and brainstem (Hosseini & Lifshitz, 2009).

In this study, the midline fluid percussion injury model was elected for use due to its ability to replicate mild and diffuse brain injury. Specifically, mFPI has been shown to produce acute behavioral deficits, the late onset of behavioral morbidities, and the absence of gross histopathology (Rowe et al, 2018). Conversely, the lateral and mid-sagittal fluid percussion injury models are effective at producing focal injuries, which are phenotypically characterized by contusions and are generally detectible on CT scans and MRIs. However, these are not as effective at replicating diffuse injuries. In this study, six brain regions were evaluated in the histopathological analyses: the cortex, the corpus callosum, the hippocampus, the thalamus, the hypothalamus, and the amygdala.

Rotarod Task

Sensorimotor function was assessed using the Economex Rotarod system from Columbus Instruments (Columbus, OH). Mice were acclimated three days prior to surgery/injury. The mice were placed on the stationary rod and allowed to explore for 30 seconds. Following exploration, the mice were placed on the rod at a constant speed of five revolutions per minute (rpm). If the mouse fell off the rod, it was placed back on the rod and the timer was restarted (until the mice could walk 15 seconds at five rpm). Next, mice were placed on the rod with an initial rotation speed of five rpm and an acceleration of 0.2 rpm/sec. The trial ended when the mouse fell off the rod; the acclimation period ended after two trials. Following acclimation, mice were trained over three consecutive days prior to surgery/injury and the last training session was recorded as baseline. Testing occurred at 2-, 5-, and 7-days post-injury (DPI). For the training and testing phase, mice were placed on the stationary rod and the motor was started at five rpm with an acceleration of 0.2 rpm/sec. Two trials were run back-to-back, and mice were returned to cages thereafter. After 10 minutes, mice preformed a third trial. Time spent on the rotarod from the best two trials were averaged to generate a time score for each mouse (Rowe et al., 2014).

Neurological Severity Score (NSS)

In 1995, Shohami and colleagues developed the Neurological Severity Score (NSS) as an assessment tool to evaluate the clinical status of rodent models in experimental TBI studies (Shohami et al., 1995). While the rotarod is useful for determining gross motor deficits in the rodent, the detection of more subtle motor effects requires an approach like the NSS. Fine motor coordination can be assessed using a beam walking or balance task. This test is designed to examine the ability of the animal to remain upright and to walk on

an elevated and relatively narrow beam (Curzon P, Zhang M, Radek RJ, et al). Our methods have been adapted from these previous works to carry out similar functions. Post-traumatic neurological impairments were assessed using an eight-point NSS paradigm. One point was given for failure on an individual task, whereas no points were given if a mouse completed a task successfully. Mice were observed for hind limb flexion, startle reflex, and seeking behavior (presence of these behaviors was considered successful task completion). Mice traversed in sequence, three, two, and one-centimeter beams. The beams were elevated and mice were given one minute to travel 30 centimeters along the beams. The task was scored as a success if the mouse traveled 30 centimeters with normal forelimb and hindlimb position (forelimb/hindlimb did not hang from the beam). Mice were also required to balance on a 0.5-centimeter beam and a 0.5-centimeter round rod for three seconds in a stationary position with front paws between hind paws. The resulting non-parametric data are presented as a composite score ranging from 1-8. A high NSS score is indicative of task failure and is interpreted as neurological impairment.

Novel Object Recognition Task (NOR)

The Novel Object Recognition Task (NOR) occurred on days 7, 14, and 28. For this task, two identical objects were placed in the arena 6 × 6 centimeters away from two different corners. The test consisted of three phases: habituation, training, and testing. On the day of the test, mice were placed in an open field (42 × 21 × 21 cm) for 1 h of habituation. Mice were then given five minutes to investigate the arena and the objects

freely for five minutes. After the mice were tested, they were returned to the housing room while the 4 hour inter-trial interval (ITI elapsed). After the ITI, a novel object replaced one of the previously explored objects and time spent with both objects was recorded. The mice were tracked using an overhead camera, and any subsequent movements was analyzed using EthoVision XT 10 software. Time spent with each object as well as the total number of visits with each object was recorded by the software and then manually checked by an investigator. Memory for object location is reflected by rats spending, on average, significantly more than 50% of investigation time with the novel object. This discrimination index was calculated by using the following equation:

Figure 3: Novel object recognition task. Mice were given 5 mins to observe identical objects placed in an open field arena. Following a 4-hour inter-trial interval, mice were placed back in the arena with one familiar object and one novel object. Time spent with the novel and familiar object was recorded and a discrimination index was calculated.

$$\frac{(Time\ spent\ with\ novel\ object - Time\ spent\ with\ familiar)}{(Time\ spent\ with\ novel\ object + Time\ spent\ with\ familiar)}$$

Forced Swim Task (FST)

The Forced Swim Task (FST) is an assay used to assess depressive-like behavior. This test involves placing the animal in a container filled with water. The assumption is that the animal will first make efforts to escape but will eventually exhibit immobility—which can be interpreted as behavioral despair. This test has been used extensively because it involves exposing the animal to stress—which has been demonstrated to play a significant role in the tendency towards major depression.

For this assay, mice were placed into glass cylinders (15 cm diameter × 24.5 cm H) filled with water (25°C) for six minutes. The first minute was excluded from analysis as an acclimation phase. Mice were visually recorded using an overhead camera. Videos were analyzed using EthoVision XT 10 software (Noldus Information Technology) for time spent actively swimming and time spent immobile. Immobility is associated with depressive-like behavior (Rowe et al., 2019).

Brain Harvest and Block Fixing

After the last day of behavioral testing, mice were euthanized, and the brain was processed for immunohistochemistry. Each mouse was over-dosed with sodium pentobarbital and transcardially perfused with 4% paraformaldehyde/phosphate buffer saline (PBS). The brains were rapidly removed. On ice, the brain was bisected along the sagittal plane with one hemisphere further dissected and flash frozen in liquid nitrogen and stored at −80°C for subsequent biochemical evaluation (Rowe et al., 2014).

Immunohistochemistry

To stain, tissue sections underwent a 10 minute high temperature antigen retrieval step and incubated with scFv-phage (1:1000) for 1 hour, then incubated with anti-M13 mouse antibody (Invitrogen 1:4000) for 1 hour. Then sections were washed and incubated with biotinylated anti-mouse IgG horse antibody (1:1000). Following washing, the Vectastain ABC-HRP kit (Vector Laboratories, Burlingame, CA) was applied. Samples were visualized using 3,3′-diaminobenzidine (DAB) as a substrate (Vector Laboratories). The sections counterstained with hematoxylin (Sigma-Aldrich).

Image data was collected using a Leica TCS SP5 LSCM in the Regenerative Medicine Imaging Facility at ASU.

ImageJ analysis

To quantitatively analyze antibody binding by region, ImageJ software (National Institute of Health, https://imagej.nih.gov/ij/) was used. Specifically, the "freehand" tool was used to draw over each designated brain region of interest (cortex, corpus callosum, hippocampus, thalamus, hypothalamus, or amygdala) to determine staining intensity in each region. These intensity reading were placed into Microsoft Excel for calculation of averages and standard deviations by group.

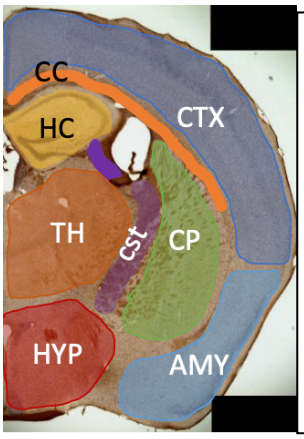

Figure 4: Map of selected brain regions for detection of staining intensity Each region above was selected for staining intensity using the ImageJ free hand tool. Of note, caudoputamen and corticospinal tract were omitted from analysis.

Statistics

For statistical analysis, there were three different sets of data prepared. The individual data from each behavioral task (NSS, NOR, FST, and Rotarod) were averaged. Next, a two-way ANOVA was performed to compare behavioral assay performance by injury group. For analysis of ImageJ staining intensity by region, SPSS software was used for one-way ANOVA tests to compare staining intensity per brain region by injury group. Lastly, behavioral findings were correlated to staining intensity using the Pearson correlate tool on SPSS. This tool aims to correlate staining intensity of ADTDP3 by region to the other behavioral assays that were performed.

CHAPTER 3

RESULTS

Diffuse TBI-induced motor deficits were measured by the Rotarod task as described in "Methods". A two-way ANOVA indicated that there was a significant time effect ($F_{(2,98)} = 21.97$; $p < 0.0001$) and injury effect ($F_{(3,\ 49)} = 22.92$; $p < 0.0001$) on motor performance. Tukey's Post-hoc test indicated that both TBI and rTBI groups exhibited a significantly shorter latency (propensity to stay on the rod) compared to the sham group (Figure 5).

Rotarod

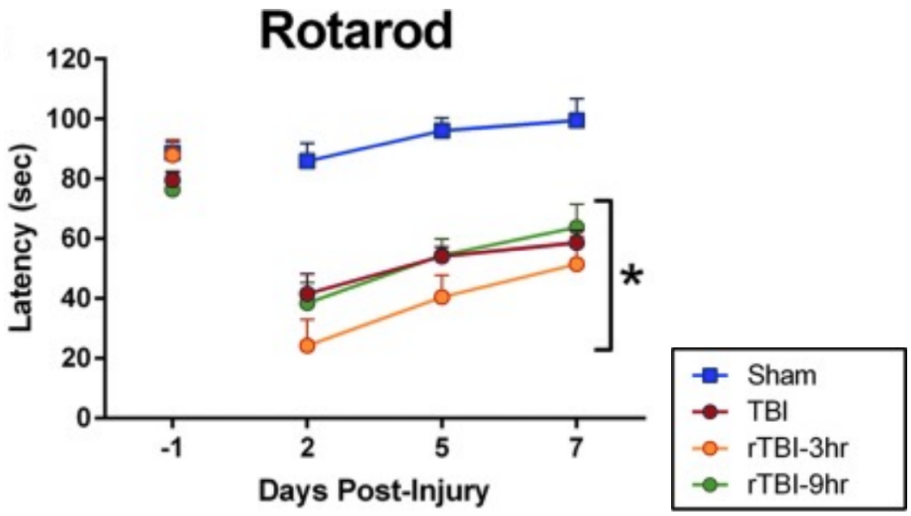

Figure 5: Rotarod task results. Diffuse TBI induced motor deficits measured by the rotarod task. There was a significant effect of time after injury on motor performance ($F_{(2,98)} = 21.97$; $p < 0.0001$). There was also a significant group effect on latency to stay on the rod ($F_{(3,\ 49)} = 22.92$; $p < 0.0001$). Tukey's post-hoc test indicated that compared to uninjured shams, all brain-injured groups demonstrated significantly shorter latencies to fall from the rotarod (Rowe et al., 2019).

Sensorimotor functional deficits were assessed using a variety of balance-related physical tests as described in "Methods". A composite score on the scale of 1-8, called the Neurological Severity Score (NSS), was used as a metric for sensorimotor deficits. A higher NSS score is indicative of more severe sensorimotor deficit. A Kruskal-Wallis Rank-Sum test indicated significant time ($\chi^2_3 = 89.39$; $p < 0.001$) and group ($\chi^2_3 = 14.45$; $p = 0.002$) effects. There was a significant injury effect of sensorimotor function for TBI, rTBI-3 hours, and rTBI-9 hours compared to uninjured shams (Figure 6).

Neurological Severity Score

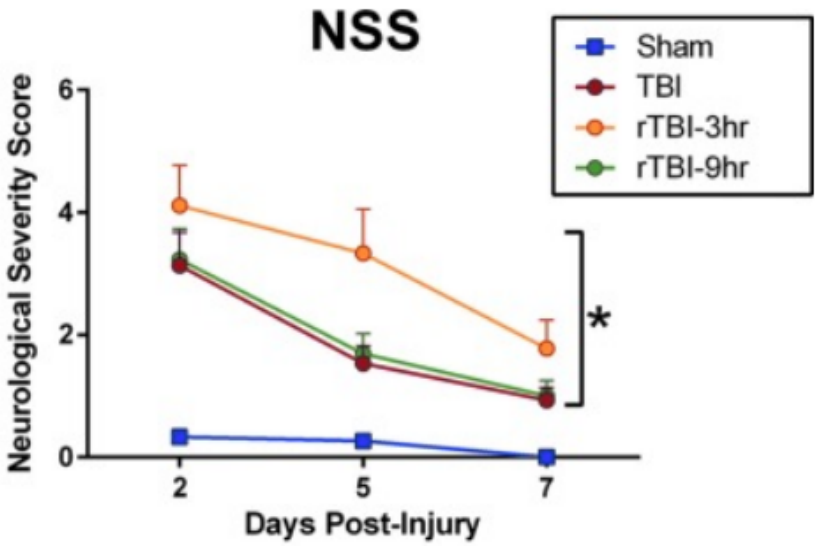

Figure 6: Neurological Severity Score results. A) Diffuse TBI induced neurological function deficits measured by a modified Neurological Severity Score (NSS). A nonparametric Kruskal-Wallis Rank-Sum test indicated significant time (($\chi^2_3 = 89.39$; $p < 0.001$) and group (($\chi^2_3 = 14.45$; $p = 0.002$) effects, with the TBI, rTBI 3 h, and rTBI 9 h groups having significantly higher NSS scores compared to uninjured shams (Rowe et al., 2019).

A one-way ANOVA indicated there was no injury effect ($F_{(3,47)} = 1.340$; $p = 0.2728$) at 7 DPI on the discrimination index calculated for NOR (Figure 7A). A one-way ANOVA indicated an overall group effect on total investigation time ($F_{(3,47} = 2.940$; $p = 0.0427$), and Tukey's multiple comparisons test indicated that the rTBI 9 h group spent significantly less time investigating objects compared to the single-TBI group (Figure 7).

Novel Object Recognition

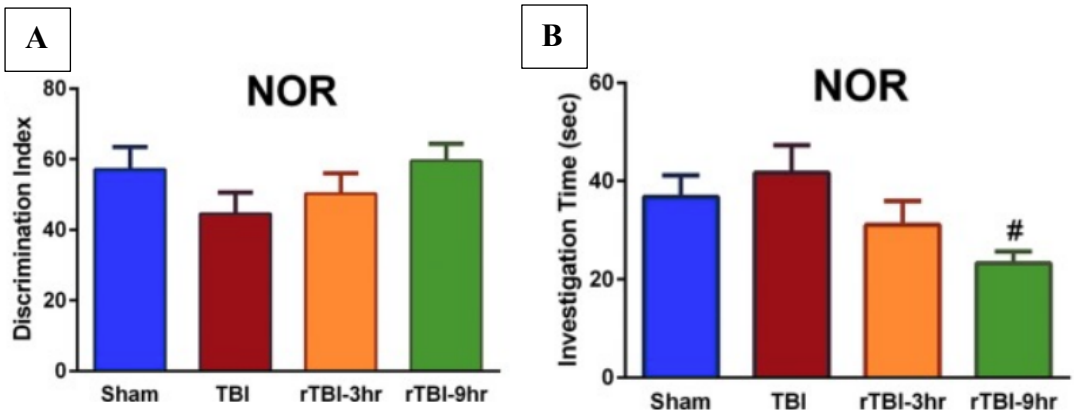

Figure 7: NOR Results. A) A one-way ANOVA indicated no overall group effect on discrimination index measured by the novel object recognition (NOR) task ($F_{(3,47)} = 1.340$; $p = 0.2728$) at 7 DPI. **B)** A one-way ANOVA indicated an overall group effect on total investigation time ($F_{(3,47} = 2.940$; $p = 0.0427$), and Tukey's multiple comparisons test indicated that the rTBI 9 h group spent significantly less time investigating objects compared to the single-TBI group. *Indicates significance from sham; #indicates significance from TBI (mean ± SEM; sham, $n = 16$; TBI, $n = 15$; rTBI 3 h, $n = 9$; rTBI 9 h, $n = 13$). **C)** Box and whisker plots depicting Novel Object Recognition task performance in Week 1, Week 2, and Week 4 cohorts, respectively. All data are compared against sham negative

Forced Swim Task

The forced swim task aims to evaluate depressive behavior. As described in Methods, time spent immobile is indicative of depressive-like behavior. A one-way

ANOVA indicated no overall group effect on time spent immobile during a forced swim task (Figure 8).

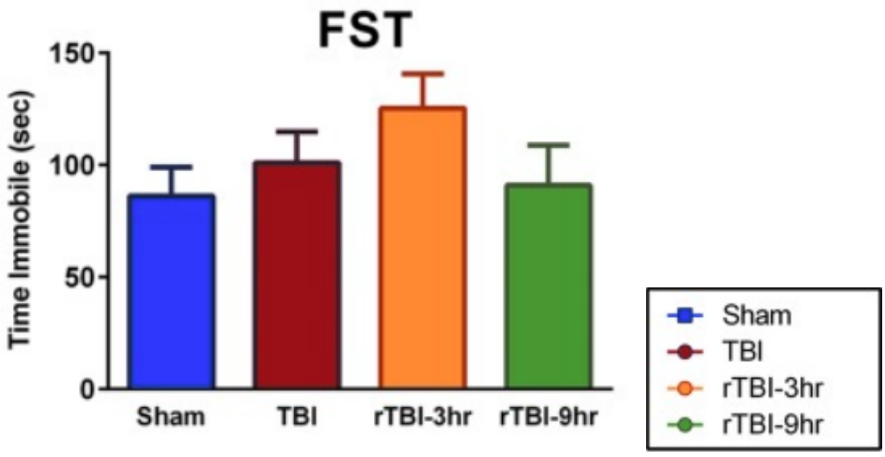

Figure 8: Forced Swim Task results. A) A one-way ANOVA indicated no overall group effect on time spent immobile during a forced swim task (FST; $F_{(3,40)} = 1.166$; $p = 0.3347$) (Rowe et al., 2019). **B)** Box and Whisker plot depicting time spent "immobile" in seconds. 14 day animals are absent from FST week 4, while 7 day animals are absent from Weeks 2 and 4 since they were sacrificed at time points prior to behavioral testing.

Next, Image J analysis was used to measure mean staining intensity by brain region and IBM SPSS was used to conduct one-way ANOVA. First, the staining intensity for each group was averaged to a single value. Then, these numbers were compared against their sham counterparts in the one-way ANOVA. A one way ANOVA indicated that there was a significant injury effect on the staining intensity of cortex (rTBI-9 hr 7 day), corpus callosum (rTBI-9 hr 7 day, TBI-28 day), thalamus (rTBI-9 hr 7 day, rTBI-9 hr 14 day), hypothalamus (rTBI-9 hr 7 day), and amygdala (TBI-28 day) compared to sham (Figure 9).

ADTDP3 Staining Intensity

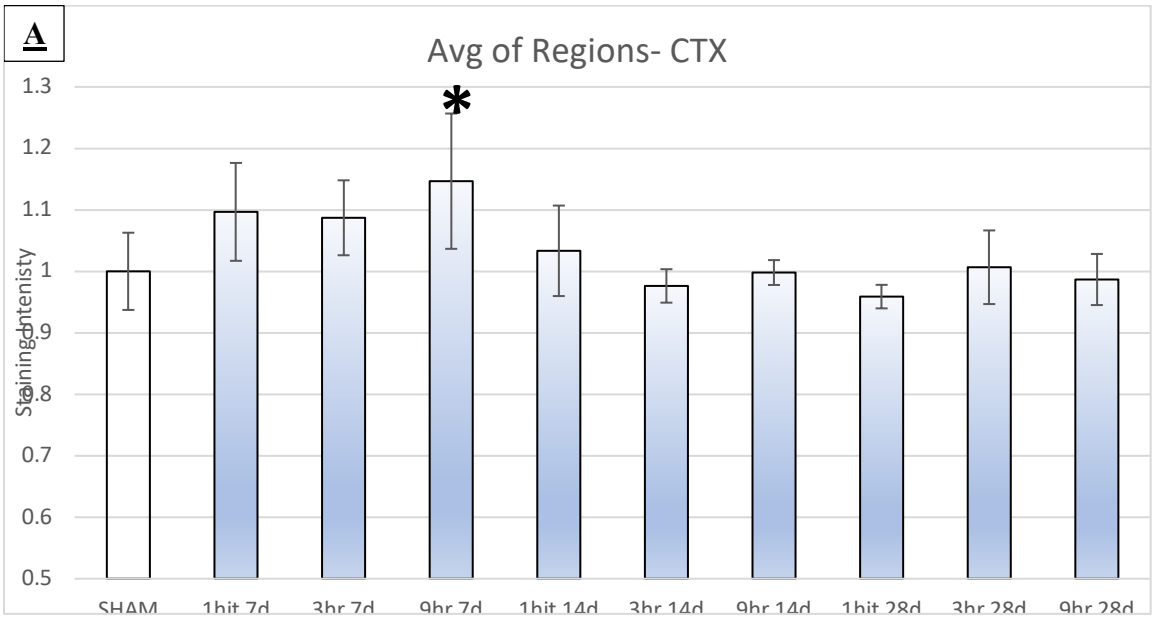

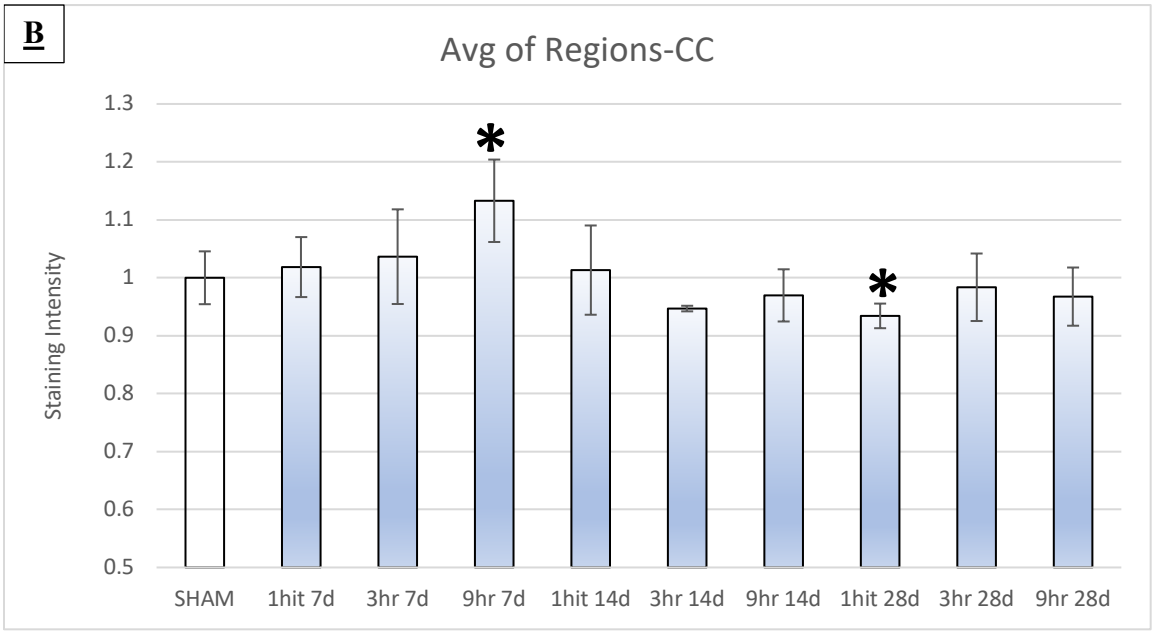

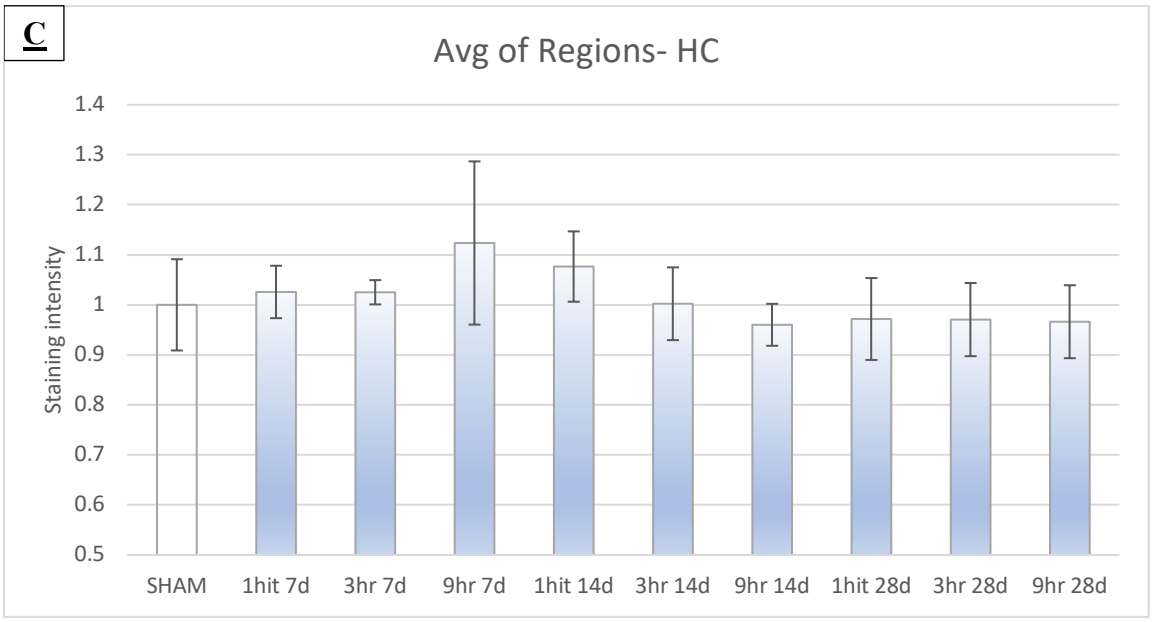
C
Avg of Regions- HC
Staining intensity
1.4
1.3
1.2
1.1
1
0.9
0.8
0.7
0.6
0.5
SHAM
1hit 7d
3hr 7d
9hr 7d
1hit 14d
3hr 14d
9hr 14d
1hit 28d
3hr 28d
9hr 28d

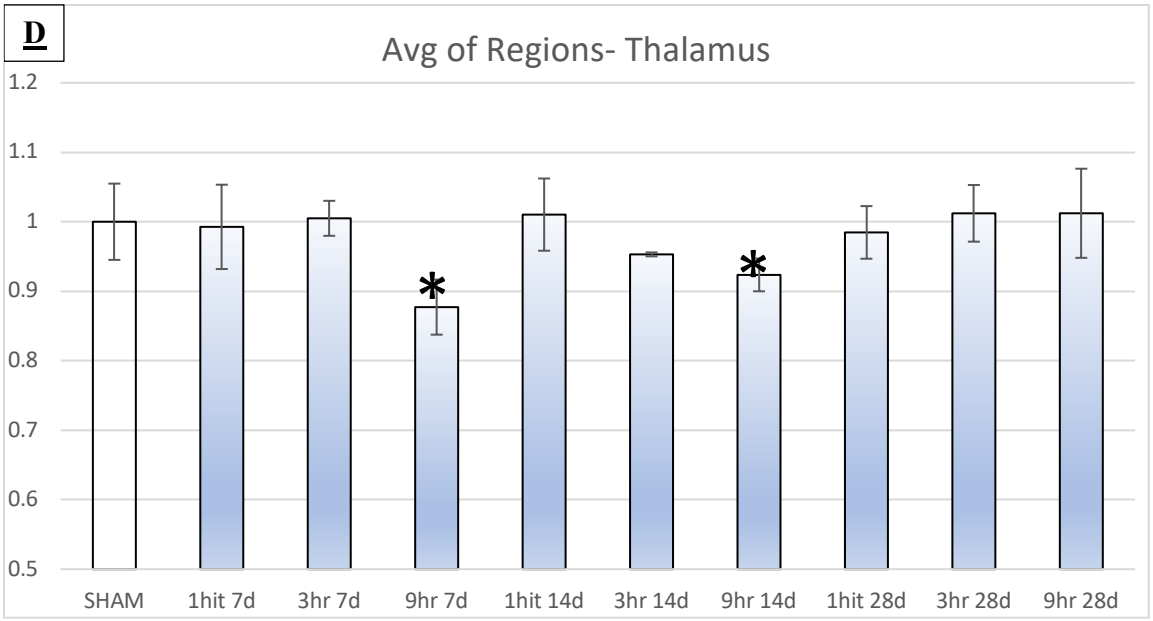
D
Avg of Regions- Thalamus
1.2
1.1
1
0.9
0.8
0.7
0.6
0.5
*
*
SHAM
1hit 7d
3hr 7d
9hr 7d
1hit 14d
3hr 14d
9hr 14d
1hit 28d
3hr 28d
9hr 28d

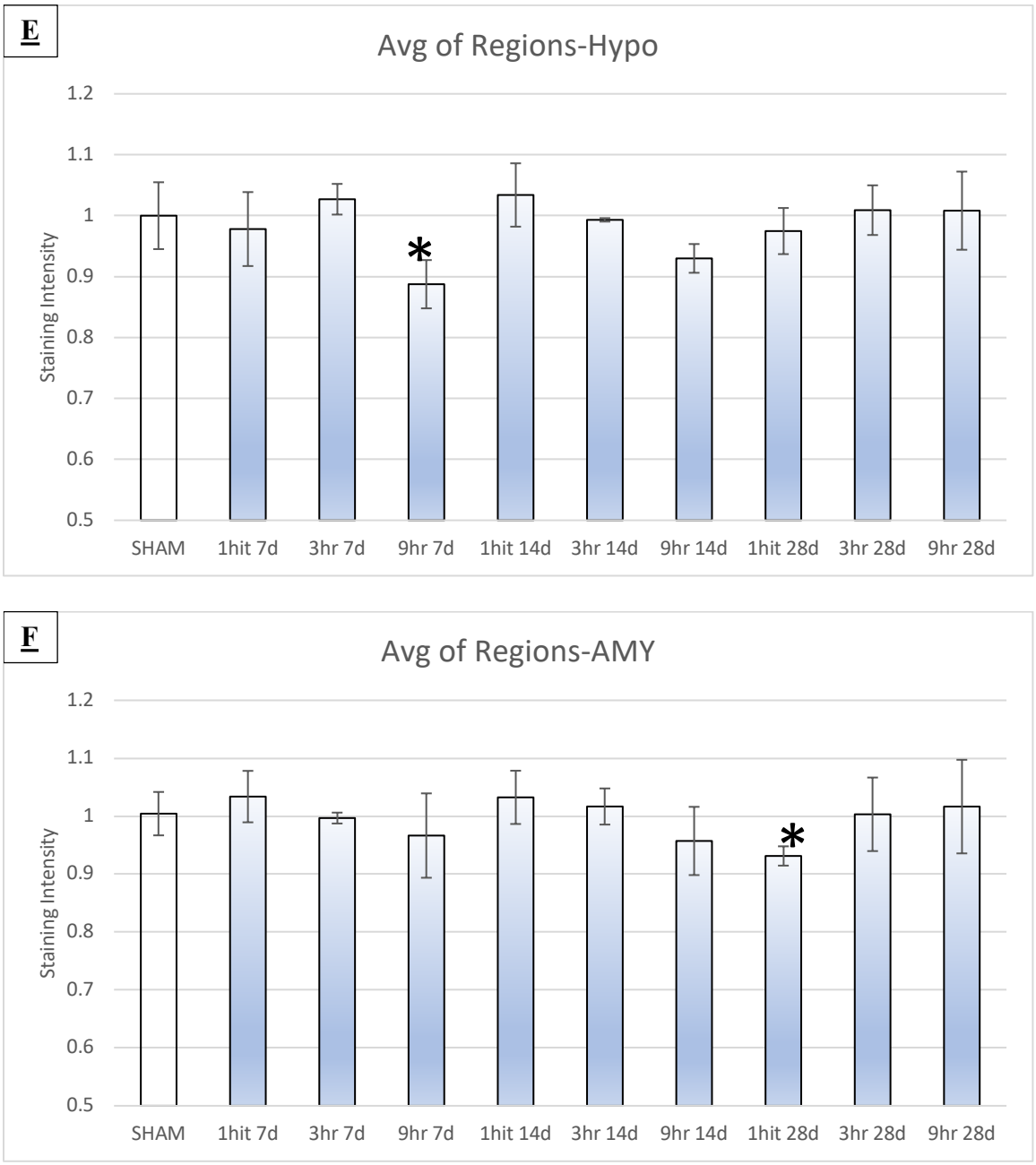

Figure 9: ADTDP3 Staining Intensity by Region. ADTDP3 antibody staining intensity in the **A)** cortex **B)** corpus callosum **C**) hippocampus **D**) thalamus **E)** hypothalamus **F**) amygdala grouped by injury and days post injury (DPI). Values are normalized to sham average value (*$p \leq 0.05$). Error bars are SD

Additionally, tissue samples at both 4× and 40× taken from fluorescence microscope are shown below (Figure 10). These representative images provide further visual aid to illustrate the significant differences in staining intensity between the sham and the 2 hit-9 day 7 DPI injury group. The 40× images particularly help illustrate the higher staining intensity within the 2 hit-9 hour 7 DPI vs sham.

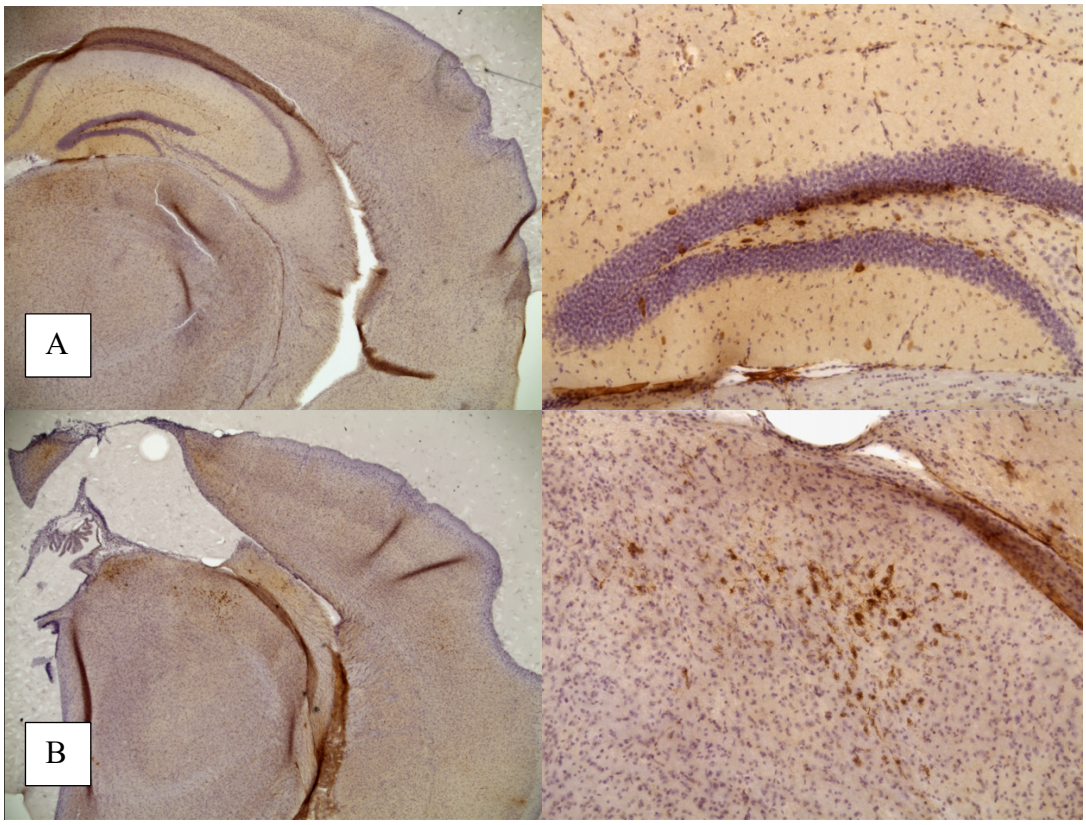

Figure 10: Representative Tissue Samples of Significant Staining in Cortex. A) Left: 4× image of sham brain tissue captured on fluorescent microscope and stitched together to construct full image. Right: 40× image of representative sham staining intensity. Dark-colored marks are indicative of ADTDP3 staining, while purple marks are nuclei and granules from H&E stain. **B)** Left: 4× image of 2 hit 9 hr DPI brain tissue captured on fluorescent microscope and stitched together to construct full image. Right: 40× image of representative 2 hit 9 hr DPI staining intensity. Dark-colored marks are indicative of ADTDP3 staining, while purple marks are nuclei and granules from H&E stain.

Behavior Correlations

Next, the Pearson Correlation function on SPSS was used to compare staining intensity between the behavioral task with staining intensity by region. There was significant correlation between CTX staining intensity and Week 1 NOR ($p = .045$; Figure 11). There were no other significant correlations between any behavioral assay with ADTDP3 staining intensity.

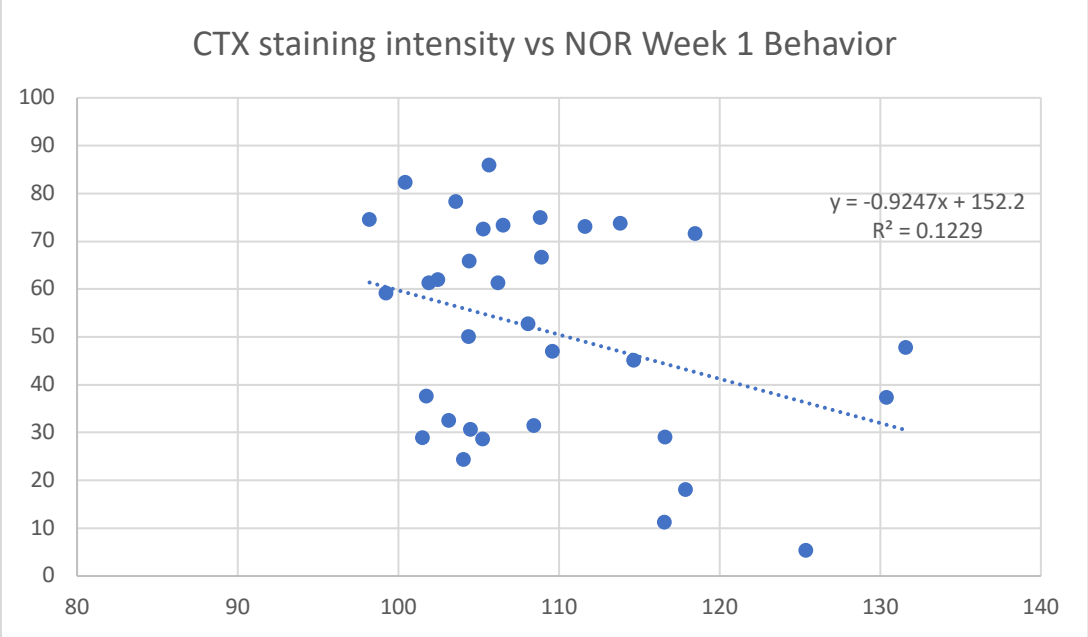

Figure 11: Cortex Staining Intensity correlation to NOR. IBM SPSS PEARSON CORRELATE function used to correlate NOR Week 1 Behavior Results to CTX staining intensity (*$p \leq 0.05$). Error bars are SD.

CHAPTER 4

DISCUSSION

Our findings suggest that TBI may influence the accumulation of toxic oligomeric variants of TDP-43 in the cortex, corpus callosum, thalamus, hypothalamus, and amygdala.

Additionally, these findings suggest that toxic oligomeric variants of TDP-43 may play a causative role in cognitive deficits secondary to TBI. These are further discussed in the context of each specific aim:

Specific Aim 1

The first aim was to identify the AD/ADRD-related protein variant fingerprint as a function of sex and time following experimental diffuse TBI. Immunohistochemistry using ADTDP3 was performed to determine if there were elevated levels of TDP-43 in TBI and r-TBI tissue compared to sham at various time points. One-way ANOVAs were performed to determine if staining intensity by region differed between sham and the respective injury groups. The cortex had significantly elevated staining intensity in the 2 hit-9 hours apart/7-day group compared to sham ($*p \leq 0.05$). It was noted that ADTDP3 preferentially recognized earlier variants of TDP-43, while some of the other scFvs recognized variants that present much later. Therefore, this finding is consistent with the preliminary data provided. In the context of an immunological response to diffuse TBI, there are also compelling biological reasons for elevated toxic TDP-43 in the cortex at this time point. The first week proceeding TBI is characterized by the pro-inflammatory phase of the immune response (Petty, 2002). Here, microglia and astrocytes assume their "activated" morphologies. This includes the release of cytokines that make the BBB leaky—which allows for the recruitment of immune cells like macrophages, lymphocytes, neutrophils, and dendritic cells (Needham et al., 2019). Microglia, macrophages, and neutrophils engage in both phagocytosis and pinocytosis to decompose cellular debris from mechanical shearing of axons and necrotic cell death (Needham et al., 2019). This process can occur

for over a week, and once this phase is complete, necrotic cell debris and potential toxic variants should be removed (Needham et al., 2019). Tissue collected at 7 DPI may likely still be in the pro-inflammatory phase. This would suggest that cellular debris and potential toxic variants of proteins stemming from mechanical damage would exist at a higher proportion (Pavlova et al., 2018). Additionally, there may be a higher density of neurons at this time post-injury since mass apoptosis secondary to neuronal atrophy does not occur until after the inflammatory phase (Petty, 2002). Lastly, r-TBI is hypothesized to have an increased inflammatory response to injury due to recent cell priming (Bailes et al., 2014). This may explain why the r-TBI groups consistently showed higher ADTDP3 staining intensity over time for nearly all brain regions evaluated.

There were significantly lower amounts of ADTDP3 staining intensity in the corpus callosum (1 hit 28 day), thalamus (9 hr 7 day, 9 hr 14 day), hypothalamus (9 hr 14 day), and amygdala (1 hit 28 day) compared to the sham group. The 14- and 28-day time points are well after the pro-inflammatory phase of the immunological response to TBI (Needham et al., 2019). Additionally, neuronal atrophy and synaptic dysfunction stemming from mechanical injuries lead to the apoptosis of several neurons after TBI (Zhou et al., 2012). The significantly lower amounts of ADTDP3 in the thalamus at an early time point can be explained, in part, by the neuroanatomy of mFPI. The midline lies above the cortex, corpus callosum, and hippocampus. This makes the mFPI likely to exert mechanical force on these brain regions at a far greater sum than in the thalamus, hypothalamus, and amygdala—or regions that lie far from the midline. If mechanical damage is proportional to mechanical force exerted, then there is less of a likelihood of exacerbated injury from the pro-

inflammatory response to TBI in the areas farther from the midline. As a result of having fewer damaged neurons, there is less of a likelihood of neuronal atrophy and dysfunction secondary to injury in the thalamus and hypothalamus. Therefore, one explanation for the significantly lower binding at this time frame is that any potential toxic variants that existed at baseline were eliminated by the immune system (Griffiths et al., 2007). As a result, this leaves the concentration of toxic TDP-43 variants in injury groups to be significantly lower than that of sham groups for the days of the inflammatory phase.

Specific Aim 2

The second aim was to determine if the staining intensity of toxic oligomeric variants found in the brain were associated with cognitive and motor deficits. The various behavioral assays demonstrated that there were significant cognitive, behavioral, and sensorimotor deficits in both TBI and r-TBI animals compared to shams. In the NSS and Rotarod tasks, this especially seemed to be true on the earlier days of testing compared to the later. A plausible cause of this difference is the influence immunological rehabilitation over time. Neuroinflammation characterizes the early days of the physiological response to primary injury, and the early removal of cellular debris and induced apoptosis for damaged cells (Needham et al., 2019). Additionally, the structural and functional refinement and remodeling neuronal connections at the synapse is occurring every time the mice ambulate or use try to use their sensorimotor abilities. Therefore, the consistent ambulation and repetition of each sensorimotor task on days 2 and 5 could be responsible for synaptogenesis—ameliorating the TBI mice's sensorimotor performance deficits significantly by day 7 (Merzenich et al., 2014). Additionally, improvement over time is

consistent with histological findings of staining intensity. For example, the cortex, corpus callosum, and hippocampus returned to sham/baseline levels after 14 DPI.

There was a significant correlation between cortex staining intensity and week 1 NOR behavior, but this significant correlation waned in NOR week 2 and NOR week 4. The neocortex has been demonstrated to play critical roles in short term memory functions—specifically in working memory and episodic memory. Funahashi and colleagues showed that spatial information has been used to understand the neural mechanism for monitoring its own operations, and it has been shown that monitoring the quality of spatial information represented by prefrontal activity is an important factor in the subject's choice (Funahashi, 2017).

Future Directions

Future directions for this project should aim to explore how other scFvs against TDP-43 fluctuate in mice with TBI and rTBI. The biopanning protocol described from Williams et al., 2017 was used to generate multiple ADTDP-specific scFvs that bind to toxic variants that arise at both earlier and later time points in disease pathology (Williams et al., 2017). These analyses need to be repeated using those primary scFvs to illustrate a more holistic picture of how TBI influences the accumulation of toxic oligomeric variants of TDP-43. This can also allow a view of how accumulation of toxic TDP-43 variants fluctuate both spatially and temporally. Toxic variants of TDP-43 are known to spread pathology throughout the brain due to their unique molecular characteristics (Guo and Shorter, 2017), so evaluating this evolution may be especially useful.

Another element to consider is how TDP-43 staining intensities and behavioral correlations compare to to scFvs made against other potential toxic protein variants. Data collected in the Sierks lab for scFvs against beta-amyloid have shown similar data to what is displayed here—with significantly elevated levels of staining intensity in the cortex, corpus callosum, and hippocampus at earlier time points. There is also a return to baseline at later time points (>14 DPI). This is further illustrated in Appendix C. At this moment, more data and analyses need to be conducted with scFvs for tau and a-syn to illustrate a holistic picture of how toxic protein levels vary over time and region.

Other genetic and environmental risk factors must be considered in future studies to explore potential synergistic effects. For example, polymorphisms in the apolipoprotein E (APOE) have been identified as major genetic risk determinants for Alzheimer's Disease, with *APOE4* elevating risk of AD and *APOE2* conferring a decreased risk relative to *APOE3* (Yamazaki et al., 2019). Strong evidence suggests that *APOE4* increases the risk of AD by driving earlier and more abundant amyloid pathology in the brain of *APOE4* carriers (Yamazaki et al., 2019). Since 25% of people carry the *APOE4* mutation (Yamazaki et al., 2019), there is great incentive to study if such genetic determinants can have synergistic effects in disease pathology. Specifically, scFvs against variants of beta amyloid are worthwhile to explore for synergistic effects due to the *APOE4* gene's direct contribution to beta amyloid-mediated disease pathology. A significant environmental risk factor to consider is obesity (Pegueroles et al., 2018). Specifically, obesity has been linked to neuronal atrophy in later stages of life. Pathological alterations such as insulin resistance, inflammation, and mitochondrial dysfunction are thought to be contributory to this

correlation (Pegueroles et al., 2018). The high incidence rate of obesity in the United States coupled with the projected increase of elderly population in the coming decades provides strong incentive to explore if obesity and TBI can have synergistic effects in causing Alzheimer's pathology. As mentioned in "Introduction", metabolic dysregulation caused by TBI can directly contribute to the formation of toxic protein variants that may cause neurodegenerative disease, so it is likely that elevated metabolic dysregulation from such a comorbidity could cause worsened neurodegenerative disease onset and pathology.

CHAPTER 5

CONCLUSION

This study provides support for the hypothesis that the accumulation of toxic variants of TDP-43 can contribute to neurodegenerative pathology and loss of function. There is a significant increase in the toxic oligomeric variants of tau bound by ADTDP3 in the cortex and corpus callosum. There is also a significant decrease in these toxic variants of TDP-43 in later time points of immunohistochemical staining. Altogether, this provides evidence that toxic oligomeric variants of TDP-43 may contribute to behavioral deficits secondary to diffuse experimental TBI. There is a strong correlation between cortex staining intensity and NOR Week 1 behavior, but this correlation fades over NOR week 2 and NOR week 4. There is reasonable neuroscientific justification for this correlation, as the cortex is known to play a critical role in short term memory and learning. Injury-induced cognitive deficits significantly correlating with elevated intensity staining indicate a high causal probability. Additionally, the neuroinflammatory effects of TBI in areas like the thalamus and hypothalamus—which are comparatively less affected by experimental diffuse mFPI—may still be experiencing an inflammatory response to remove and dispose of potential toxic variants of proteins. This could sufficiently explain the significantly lower amounts of toxic protein variants being seen in these areas relative to sham. Future directions of this study include using other TDP-43-specific scFvs that preferentially bind at later timepoints to illustrate a more holistic picture.

These findings also offer clinical utility. There is a significant clinical need for effective biomarkers for neurodegenerative diseases like AD (Sharma and Singh, 2016).

Although beta amyloid plaques and neurofibrillary tangles have been considered the histological pathologies indicative of neurodegenerative disease, they do not serve as effective biomarkers because they are not predictive of the onset of neurodegenerative disease (Lee, Kim, Hong et al., 2019). Compelling cases have been made for toxic oligomeric variants of proteins like TDP-43, tau, a-syn, and b-amyloid to serve as better biomarkers to predict onset of neurodegenerative disease, though more research must be performed to confirm this. The Sierks lab at Arizona State University has generated scFvs specific to various toxic oligomeric variants of each of these respective proteins (Williams et al., 2017). Clinically, these scFvs could be used in a laboratory panel to determine a patient's risk for neurodegenerative disease. Here, a patient's cerebrospinal fluid or serum could be collected at various time points after TBI, repetitive TBI, or any other identified risk factor to monitor for fluctuations in levels of these toxic protein variants. Such a panel could serve as a clinically useful tool for assessing risk for neurodegenerative disease and constructing patient specific plans of care to mitigate the likelihood of these developments. Lastly, this scFvs engineering protocol could serve as a pipeline for future protein engineering therapeutics projects for direct clinical treatment. This AFM-based protocol allows for the exploration of specific molecular interactions due to its ability to operate at the scale of nanometers. Therefore, future directions could include the exploration of allosteric binding or regulation to directly mitigate the spreading of toxicity from these toxic protein variants.

REFERENCES

1. Agarwal, Nitin, et al. “Traumatic Brain Injury.” *AANS*, American Association of Neurological Surgeons, www.aans.org/Patients/Neurosurgical-Conditions-and-Treatments/Traumatic-Brain-Injury.

2. Champion, Howard R. MD, FRCS, FACS; Holcomb, John B. MD, FACS; Young, Lee Ann MA Injuries From Explosions: Physics, Biophysics, Pathology, and Required Research Focus, The Journal of Trauma: Injury, Infection, and Critical Care: May 2009 - Volume 66 - Issue 5 - p 1468-1477 doi: 10.1097/TA.0b013e3181a27e7f

3. Pearn, M.L., Niesman, I.R., Egawa, J. *et al.* Pathophysiology Associated with Traumatic Brain Injury: Current Treatments and Potential Novel Therapeutics. *Cell Mol Neurobiol* **37,** 571–585 (2017). https://doi.org/10.1007/s10571-016-0400-1

4. Aniessen, T. M. J. .., et al. “Clinical Characteristics and Pathophysiological Mechanisms of Focal and Diffuse Traumatic Brain Injury.” *Journal of Cellular and Molecular Medicine*, vol. 14, no. 10, Blackwell Publishing Ltd, 2010, pp. 2381–92, doi:10.1111/j.1582-4934.2010.01164.x.

5. Gaugler, Joseph, et al. “2018 Alzheimer's Facts and Figures.” *Alz.org*, Alzheimer's Association, www.alz.org/media/homeoffice/facts%20and%20figures/facts-and-figures.pdf.

6. H Braak, E Braak, Diagnostic Criteria for Neuropathologic Assessment of Alzheimer’s Disease, Neurobiology of Aging,Volume 18, Issue 4, Supplement 1,1997,Pages S85-S88,ISSN 0197-4580, https://doi.org/10.1016/S0197-4580(97)00062-6.

7. Rohn, Troy T. “Cytoplasmic inclusions of TDP-43 in neurodegenerative diseases: a potential role for caspases.” *Histology and histopathology* vol. 24,8 (2009): 1081-6. doi:10.14670/HH-24.1081

8. E.J. Needham, A. Helmy, E.R. Zanier, J.L. Jones, A.J. Coles, D.K. Menon The immunological response to traumatic brain injury J. Neuroimmunol., 332 (2019), pp. 112-125

9. Hyder, Adnan A. et al. ‘The Impact of Traumatic Brain Injuries: A Global Perspective’. 1 Jan. 2007 : 341 – 353

10. "Traumatic Brain Injury." *AANS*, www.aans.org/Patients/Neurosurgical-Conditions-and-Treatments/Traumatic-Brain-Injury.

11. Blennow, K., Brody, D. L., Kochanek, P. M., Levin, H., McKee, A., Ribbers, G. M., . . . Zetterberg, H. (2016). Traumatic brain injuries. *Nat Rev Dis Primers, 2*, 16084. doi:10.1038/nrdp.2016.84

12. Sharma, Neeti, and Anshika Nikita Singh. "Exploring Biomarkers for Alzheimer's Disease." *Journal of clinical and diagnostic research : JCDR* vol. 10,7 (2016): KE01-6. doi:10.7860/JCDR/2016/18828.8166

13. Mckee, Ann C, and Daniel H Daneshvar. "The neuropathology of traumatic brain injury." *Handbook of clinical neurology* vol. 127 (2015): 45-66. doi:10.1016/B978-0-444-52892-6.00004-0

14. Drew LB, Drew WE. The contrecoup-coup phenomenon: a new understanding of the mechanism of closed head injury. Neurocrit Care. 2004;1(3):385-90. doi: 10.1385/NCC:1:3:385. PMID: 16174940.

15. Andriessen, Teuntje M J C et al. "Clinical characteristics and pathophysiological mechanisms of focal and diffuse traumatic brain injury." *Journal of cellular and molecular medicine* vol. 14,10 (2010): 2381-92. doi:10.1111/j.1582-4934.2010.01164.x

16. Yamazaki, Y., Zhao, N., Caulfield, T.R. *et al.* Apolipoprotein E and Alzheimer disease: pathobiology and targeting strategies. *Nat Rev Neurol* **15,** 501–518 (2019). https://doi.org/10.1038/s41582-019-0228-7

17. Bryden, Daniel W et al. "Blast-Related Traumatic Brain Injury: Current Concepts and Research Considerations." *Journal of experimental neuroscience* vol. 13 1179069519872213. 12 Sep. 2019, doi:10.1177/1179069519872213

18. Jay M. Meythaler, Jean D. Peduzzi, Evangelos Eleftheriou, Thomas A. Novack, Current concepts: Diffuse axonal injury–associated traumatic brain injury, Archives of Physical Medicine and Rehabilitation, Volume 82, Issue 10 2001,Pages 1461-1471,ISSN 0003-9993,https://doi.org/10.1053/apmr.2001.25137.

19. Povlishock, John T. PhD; Katz, Douglas I. MD Update of Neuropathology and Neurological Recovery After Traumatic Brain Injury, Journal of Head Trauma Rehabilitation: January-February 2005 - Volume 20 - Issue 1 - p 76-94

20. Chen, Ruoli et al. "Reactive Oxygen Species Formation in the Brain at Different Oxygen Levels: The Role of Hypoxia Inducible Factors." *Frontiers in cell and developmental biology* vol. 6 132. 10 Oct. 2018, doi:10.3389/fcell.2018.00132

21. Iguchi Y, Katsuno M, Takagi S, Ishigaki S, Niwa J, Hasegawa M, Tanaka F, Sobue G. Oxidative stress induced by glutathione depletion reproduces pathological modifications of TDP-43 linked to TDP-43 proteinopathies. Neurobiol Dis. 2012 Mar;45(3):862-70. doi: 10.1016/j.nbd.2011.12.002. Epub 2011 Dec 13.

22. Abu Hamdeh, S., Shevchenko, G., Mi, J. *et al.* Proteomic differences between focal and diffuse traumatic brain injury in human brain tissue. *Sci Rep* 8, 6807 (2018). https://doi.org/10.1038/s41598-018-25060-0

23. Mayeux, Richard. "Epidemiology of Neurodegeneration." *Annual review of neuroscience* 26 (2003): 81–104. Print.

24. Guo, Lin, and James Shorter. "Biology and Pathobiology of TDP-43 and Emergent Therapeutic Strategies." *Cold Spring Harbor perspectives in medicine* vol. 7,9 a024554. 1 Sep. 2017, doi:10.1101/cshperspect.a024554

25. "What?: JPND." *JPND | Neurodegenerative Disease Research*, 26 Apr. 2017, www.neurodegenerationresearch.eu/what/.

26. "2018 Alzheimer's Disease Facts and Figures." *Alzheimer's & dementia* 14.3 (2018): 367–429. Web.

27. Lee, J.C., Kim, S.J., Hong, S. *et al.* Diagnosis of Alzheimer's disease utilizing amyloid and tau as fluid biomarkers. *Exp Mol Med* **51,** 1–10 (2019). https://doi.org/10.1038/s12276-019-0250-2

28. Lee, E., Lee, VY. & Trojanowski, J. Gains or losses: molecular mechanisms of TDP43-mediated neurodegeneration. *Nat Rev Neurosci* 13, 38–50 (2012). https://doi.org/10.1038/nrn3121

29. Rowe, Rachel K et al. "Recovery of neurological function despite immediate sleep disruption following diffuse brain injury in the mouse: clinical relevance to medically untreated concussion." Sleep vol. 37,4 743-52. 1 Apr. 2014, doi:10.5665/sleep.3582

30. Shohami E, Novikov M, Bass R (1995) Long-term effect of HU-211, a novel non-competitive NMDA antagonist, on motor and memory functions after closed head injury in the rat. Brain Res 674:55–62.

31. Pavlova, Velichka et al. "Pioglitazone Therapy and Fractures: Systematic Review and Meta- Analysis." *Endocrine, metabolic & immune disorders drug targets* vol. 18,5 (2018): 502-507. doi:10.2174/1871530318666180423121833 2

32. Rowe, Rachel K et al. “Recovery of neurological function despite immediate sleep disruption following diffuse brain injury in the mouse: clinical relevance to medically untreated concussion.” *Sleep* vol. 37,4 743-52. 1 Apr. 2014, doi:10.5665/sleep.3582

33. Rowe, Rachel K et al. “Acute Post-Traumatic Sleep May Define Vulnerability to a Second Traumatic Brain Injury in Mice.” *Journal of neurotrauma* vol. 36,8 (2019): 1318-1334. doi:10.1089/neu.2018.5980

34. Petty MA, Lo EH. 2002. Junctional complexes of the blood-brain barrier: Permeability changes in neuroinflammation. Prog Neurobiol 68(5): 311–323.

35. Blixt, Jonas et al. “Aquaporins and Blood–brain Barrier Permeability in Early Edema Development after Traumatic Brain Injury.” *Brain Research* 1611 (2015): 18–28. Web.

36. Bao, Hai-Jun et al. “Poloxamer-188 Attenuates TBI-Induced Blood–Brain Barrier Damage Leading to Decreased Brain Edema and Reduced Cellular Death.” *Neurochemical Research* 37.12 (2012): 2856–2867. Web.

37. Orr, Miranda E et al. “A Brief Overview of Tauopathy: Causes, Consequences, and Therapeutic Strategies.” *Trends in pharmacological sciences* vol. 38,7 (2017): 637-648. doi:10.1016/j.tips.2017.03.011

38. Brooke Fehily, and Melinda Fitzgerald. “Repeated Mild Traumatic Brain Injury.” *Cell Transplantation*, vol. 26, SAGE Publishing, 2017, doi:10.1177/0963689717714092.

39. Liu, Fei et al. “O-GlcNAcylation regulates phosphorylation of tau: a mechanism involved in Alzheimer's disease.” *Proceedings of the National Academy of Sciences of the United States of America* vol. 101,29 (2004): 10804-9. doi:10.1073/pnas.0400348101

40. Ramkumar, Amrita et al. “ReMAPping the microtubule landscape: How phosphorylation dictates the activities of microtubule-associated proteins.” *Developmental dynamics : an official publication of the American Association of Anatomists* vol. 247,1 (2018): 138-155. doi:10.1002/dvdy.24599

41. Hosseini, H., and H. Lifshitz. “Brain Injury Forces of Moderate Magnitude Elicit the Fencing Response.” *Medicine & Science in Sports & Exercise* 41.9 (2009): 1687–1697. Web.

42. Curzon P, Zhang M, Radek RJ, et al. The Behavioral Assessment of Sensorimotor Processes in the Mouse: Acoustic Startle, Sensory Gating, Locomotor Activity,

Rotarod, and Beam Walking. In: Buccafusco JJ, editor. Methods of Behavior Analysis in Neuroscience. 2nd edition. Boca Raton (FL): CRC Press/Taylor & Francis; 2009. Chapter 8. Available from: https://www.ncbi.nlm.nih.gov/books/NBK5236/

43. Yankelevitch-Yahav, Roni et al. "The forced swim test as a model of depressive-like behavior." *Journal of visualized experiments : JoVE* ,97 52587. 2 Mar. 2015, doi:10.3791/52587

44. Gavett BE, Stern RA, Cantu RC, Nowinski CJ, McKee AC. Mild traumatic brain injury: a risk factor for neurodegeneration. Alzheimers Res Ther. 2010 Jun 25;2(3):18. doi: 10.1186/alzrt42. PMID: 20587081; PMCID: PMC2919698.

45. Garcia-Sierra, F., Ghoshal, N., Quinn, B., Berry, R. W. & Binder, L. I. Conformational changes and truncation of tau protein during tangle evolution in Alzheimer's disease. *J Alzheimers Dis* **5**, 65-77 (2003).

46. Pegueroles, Jordi et al. "Obesity and Alzheimer's disease, does the obesity paradox really exist? A magnetic resonance imaging study." *Oncotarget* vol. 9,78 34691-34698. 5 Oct. 2018, doi:10.18632/oncotarget.26162

47. Nemetz, P. N. *et al.* Traumatic brain injury and time to onset of Alzheimer's disease: a population-based study. *Am J Epidemiol* **149**, 32-40 (1999).

48. Williams SM, Schulz P, Sierks MR. Oligomeric α-synuclein and β-amyloid variants as potential biomarkers for Parkinson's and Alzheimer's diseases. Eur J Neurosci. 2016 Jan;43(1):3-16. doi: 10.1111/ejn.13056. Epub 2015 Oct 15. PMID: 26332448; PMCID: PMC4718789.

49. Montalbano, Mauro et al. "TDP-43 and Tau Oligomers in Alzheimer's Disease, Amyotrophic Lateral Sclerosis, and Frontotemporal Dementia." *Neurobiology of disease* vol. 146 (2020): 105130. doi:10.1016/j.nbd.2020.105130

50. Vanden Broeck L, Callaerts P, Dermaut B. TDP-43-mediated neurodegeneration: towards a loss-of-function hypothesis? Trends Mol Med. 2014 Feb;20(2):66-71. doi: 10.1016/j.molmed.2013.11.003. Epub 2013 Dec 16. PMID: 24355761.

51. Tollervey JR, Curk T, Rogelj B, Briese M, Cereda M, Kayikci M, König J, Hortobágyi T, Nishimura AL, Zupunski V, Patani R, Chandran S, Rot G, Zupan B, Shaw CE, Ule J. Characterizing the RNA targets and position-dependent splicing regulation by TDP-43. Nat Neurosci. 2011 Apr;14(4):452-8. doi: 10.1038/nn.2778. Epub 2011 Feb 27. PMID: 21358640; PMCID: PMC3108889.

52. Buratti E, Baralle FE. The multiple roles of TDP-43 in pre-mRNA processing and gene expression regulation. RNA Biol. 2010 Jul-Aug;7(4):420-9. doi: 10.4161/rna.7.4.12205. Epub 2010 Jul 1. PMID: 20639693.

53. Rowe, Rachel K et al. "Acute Post-Traumatic Sleep May Define Vulnerability to a Second Traumatic Brain Injury in Mice." *Journal of neurotrauma* vol. 36,8 (2019): 1318-1334. doi:10.1089/neu.2018.5980

54. Wylie GR, Freeman K, Thomas A, Shpaner M, OKeefe M, Watts R, Naylor MR. Cognitive Improvement after Mild Traumatic Brain Injury Measured with Functional Neuroimaging during the Acute Period. PLoS One. 2015 May 11;10(5):e0126110. doi: 10.1371/journal.pone.0126110. PMID:

55. Funahashi, Shintaro. "Working Memory in the Prefrontal Cortex." *Brain sciences* vol. 7,5 49. 27 Apr. 2017, doi:10.3390/brainsci7050049

56. Zhou, Hongzhen et al. "Moderate traumatic brain injury triggers rapid necrotic death of immature neurons in the hippocampus." *Journal of neuropathology and experimental neurology* vol. 71,4 (2012): 348-59. doi:10.1097/NEN.0b013e31824ea078

57. Bailes JE, Dashnaw ML, Petraglia AL, Turner RC. Cumulative effects of repetitive mild traumatic brain injury. Prog Neurol Surg. 2014;28:50-62. doi: 10.1159/000358765. Epub 2014 Jun 6. PMID: 24923392.

58. M. Griffiths, J.W. Neal, P. Gasque, Innate Immunity and Protective Neuroinflammation: New Emphasis on the Role of Neuroimmune Regulatory Proteins, International Review of Neurobiology, Academic Press, Volume 82, 2007, Pages 29-55, ISSN 0074-7742, ISBN 9780123739896, https://doi.org/10.1016/S0074-7742(07)82002-2.

59. Merzenich, Michael M et al. "Brain plasticity-based therapeutics." *Frontiers in human neuroscience* vol. 8 385. 27 Jun. 2014, doi:10.3389/fnhum.2014.00385

APPENDIX

APPENDIX A

RAW PEARSON CORRELATION CALCULATIONS

		HC	RR D2 L	RR D7 L	RR D5 L	NSS D2	NSS D5	NSS D7	NOR W1 DI	NOR W4 DI	NOR W2 DI	FSM W1 Im	FST W2 Im	FST W4 Im	EPM W1 Open	
HC	Pearson Correlation	1	-.265	-.067	-.095	-.090	-.097	.014	-.212	-.107	-.217	-.042	.105	.155	-.102	
	Sig. (2-tailed)		.136	.711	.600	.618	.592	.937	.236	.716	.309	.843	.627	.597	.574	
	N	36	33	33	33	33	33	33	33	14	24	25	24	14	33	
CTX	Pearson Correlation	-.124	-.106	-.038	-.007	.082	.113	-.351*	-.113	-.037	-.088	-.297	.004	.054	1	
	Sig. (2-tailed)	.491	.559	.834	.967	.650	.530	.045	.699	.865	.677	.158	.989	.765		
	N	33	33	33	33	33	33	33	14	24	25	24	14	33	36	
TH	Pearson Correlation	.053	.021	.125	-.120	.020	-.109	-.381*	-.047	.225	.236	-.158	.065	.008	1	
	Sig. (2-tailed)	.767	.904	.481	.501	.912	.540	.026	.873	.291	.247	.460	.824	.965		
	N	34	34	34	34	34	34	34	14	24	26	24	14	33	37	
CC	Pearson Correlation	-.177	-.127	-.024	-.078	.067	.071	-.228	-.096	-.105	-.030	-.192	-.102	-.128	1	
	Sig. (2-tailed)	.359	.512	.900	.686	.728	.715	.235	.767	.651	.893	.405	.752	.508		
	N	29	29	29	29	29	29	29	12	21	22	21	12	29	32	
AMY	Pearson Correlation	.065	.141	.147	-.072	.014	.044	-.184	-.054	-.035	.091	-.157	.042	-.177	1	
	Sig. (2-tailed)	.713	.428	.407	.684	.937	.807	.297	.854	.869	.660	.465	.887	.324		
	N	34	34	34	34	34	34	34	14	24	26	24	14	33	37	
HYP	Pearson Correlation	.068	.217	.187	-.208	-.049	-.205	-.144	.098	.232	.106	-.175	-.095	.050	1	
	Sig. (2-tailed)	.703	.218	.289	.238	.784	.246	.416	.739	.276	.606	.413	.747	.784		
	N	34	34	34	34	34	34	34	14	24	26	24	14	33	37	

Figure B1: All Behavioral Correlations to Staining Intensity. Staining intensity for all brain regions compared to behavioral results for Rotarod, NSS, NOR, FST, and EPM tasks. IBM SPSS Pearson Correlation function used to compare data sets.

APPENDIX B

RAW STAINING INTENSITY BY REGION CALCULATIONS

Dependent VariableCTX

Test LSD

(I) InjuryNUM	(J) InjuryNUM	Mean Difference (I-J)	Std. Error	Sig.	95% Confidence Interval	
					Lower Bound	Upper Bound
SHAM	1 HIT 7 DAY	-.06880	.04680	.154	-.1650	.0274
	3 HR 7 DAY	-.05916	.04680	.217	-.1554	.0370
	9 HR 7 DAY	-.11874*	.05438	.038	-.2305	-.0070
	1 HT 14 DAY	-.00545	.04251	.899	-.0928	.0819
	3 HR 14 DAY	.05167	.05438	.351	-.0601	.1634
	9 HR 14 DAY	.02989	.04251	.488	-.0575	.1173
	1 HT 28 DAY	.06904	.04680	.152	-.0272	.1652
	3 HR 28 DAY	.02127	.04251	.621	-.0661	.1086
	9 HR 28 DAY	.04122	.04251	.341	-.0462	.1286

Dependent VariableCC

Test LSD

(I) InjuryNUM	(J) InjuryNUM	Mean Difference (I-J)	Std. Error	Sig.	95% Confidence Interval	
					Lower Bound	Upper Bound
SHAM	1 HIT 7 DAY	.008664	.043507	.844	-.08156	.09889
	3 HR 7 DAY	-.009297	.049844	.854	-.11267	.09407
	9 HR 7 DAY	-.105762*	.049844	.045	-.20913	-.00239
	1 HT 14 DAY	.013893	.039964	.731	-.06899	.09677
	3 HR 14 DAY	.080269	.049844	.122	-.02310	.18364
	9 HR 14 DAY	.057527	.039964	.164	-.02535	.14041
	1 HT 28 DAY	.092925*	.043507	.044	.00270	.18315
	3 HR 28 DAY	.043503	.039964	.288	-.03938	.12638
	9 HR 28 DAY	.059645	.043507	.184	-.03058	.14987

Dependent VariableHC

Test LSD

(I) InjuryNUM	(J) InjuryNUM	Mean Difference (I-J)	Std. Error	Sig.	95% Confidence Interval	
					Lower Bound	Upper Bound
SHAM	1 HIT 7 DAY	-.01277	.05288	.811	-.1215	.0959
	3 HR 7 DAY	-.01216	.05288	.820	-.1209	.0965
	9 HR 7 DAY	-.11063	.06144	.083	-.2369	.0157
	1 HT 14 DAY	-.06356	.04803	.197	-.1623	.0352
	3 HR 14 DAY	.01075	.06144	.862	-.1155	.1371
	9 HR 14 DAY	.05288	.04803	.281	-.0459	.1516
	1 HT 28 DAY	.04127	.05288	.442	-.0674	.1500
	3 HR 28 DAY	.04245	.04803	.385	-.0563	.1412
	9 HR 28 DAY	.04671	.04803	.340	-.0520	.1454

Dependent VariableTH

Test LSD

(I) InjuryNUM	(J) InjuryNUM	Mean Difference (I-J)	Std. Error	Sig.	95% Confidence Interval	
					Lower Bound	Upper Bound
SHAM	1 HIT 7 DAY	.01054	.02938	.723	-.0497	.0708
	3 HR 7 DAY	-.00175	.03235	.957	-.0681	.0646
	9 HR 7 DAY	.12606*	.03759	.002	.0489	.2032
	1 HT 14 DAY	-.00710	.02938	.811	-.0674	.0532
	3 HR 14 DAY	.05015	.03759	.193	-.0270	.1273
	9 HR 14 DAY	.07970*	.02938	.011	.0194	.1400
	1 HT 28 DAY	.01854	.03235	.571	-.0478	.0849
	3 HR 28 DAY	-.00893	.02938	.763	-.0692	.0514
	9 HR 28 DAY	-.00900	.02938	.762	-.0693	.0513

Dependent VariableHYP

Test LSD

(I) InjuryNUM	(J) InjuryNUM	Mean Difference (I-J)	Std. Error	Sig.	95% Confidence Interval	
					Lower Bound	Upper Bound
SHAM	1 HIT 7 DAY	.02832	.02567	.280	-.0244	.0810
	3 HR 7 DAY	-.02064	.02826	.472	-.0786	.0374
	9 HR 7 DAY	.11883*	.03284	.001	.0514	.1862
	1 HT 14 DAY	-.02763	.02567	.291	-.0803	.0251
	3 HR 14 DAY	.01321	.03284	.691	-.0542	.0806
	9 HR 14 DAY	.07649*	.02567	.006	.0238	.1292
	1 HT 28 DAY	.03160	.02826	.273	-.0264	.0896
	3 HR 28 DAY	-.00269	.02567	.917	-.0554	.0500
	9 HR 28 DAY	-.00186	.02567	.943	-.0545	.0508

Dependent VariableAMY

Test LSD

(I) InjuryNUM	(J) InjuryNUM	Mean Difference (I-J)	Std. Error	Sig.	95% Confidence Interval	
					Lower Bound	Upper Bound
SHAM	1 HIT 7 DAY	-.03022	.03155	.347	-.0949	.0345
	3 HR 7 DAY	.00683	.03473	.846	-.0644	.0781
	9 HR 7 DAY	.03706	.04035	.367	-.0457	.1199
	1 HT 14 DAY	-.02890	.03155	.368	-.0936	.0358
	3 HR 14 DAY	-.01311	.04035	.748	-.0959	.0697
	9 HR 14 DAY	.04637	.03155	.153	-.0184	.1111
	1 HT 28 DAY	.07228*	.03473	.047	.0010	.1435
	3 HR 28 DAY	.00036	.03155	.991	-.0644	.0651
	9 HR 28 DAY	-.01296	.03155	.684	-.0777	.0518

Figure B1: Staining Intensity by Region. Staining Intensity by region for all injury groups, normalized to sham. Using IBM SPSS, a one-way ANOVA was conducted to compare injury group values to sham values.

APPENDIX C

BETA AMYLOID SCFV CORRELATIONS

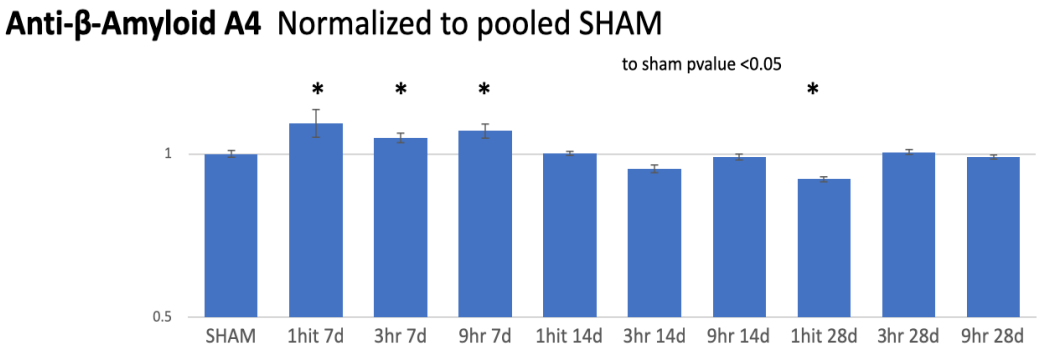

Figure C1: Anti-B-Amyloid A4 Staining Normalized to Pool sham. Staining Intensity by region for all injury groups, normalized to sham. Using IBM SPSS, a one-way ANOVA was conducted to compare injury group values to sham values. (*p ≤ 0.05).

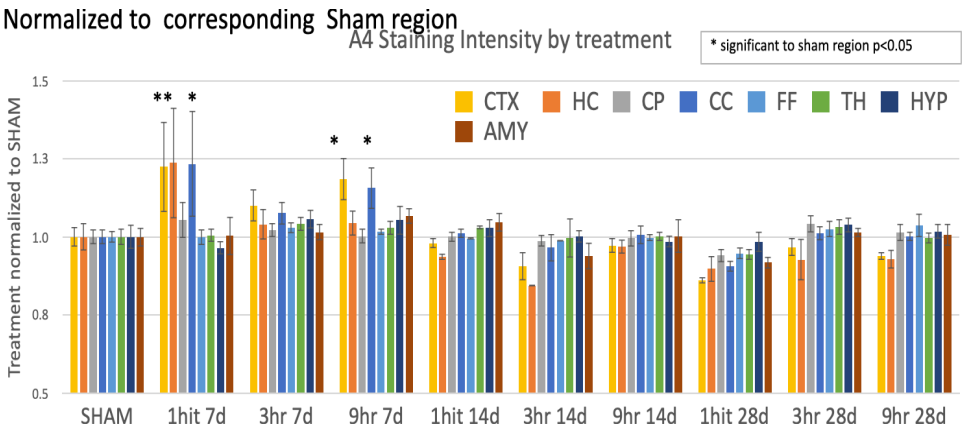

Figure C2: Treatment Normalized to Corresponding Sham Region. Representation of staining intensity by region and by injury group and timepoint DPI. (*p < 0.05). Error bars are SD.